Chapter 4
Experimental Methods for Estimating the Fluxes of Energy and Matter

In meteorology and climatology, typically only specific atmospheric variables are measured in operational networks and energy and matter fluxes cannot easily be determined. In the last 20 years, the growing interest and research on climate change has increased the demand for reliable measurements of evaporation, carbon dioxide uptake by forests, and fluxes of other greenhouse gases. So far, these measurements were primarily for research purposes but their integration into operational networks is increasing. The measurements are very complex and need comprehensive micrometeorological knowledge. Most of the measurement methods are based on simplifications and special conditions, and therefore their implementation is not trivial. In the following chapter, overview tables provide guidance to the reader about areas of applications and related costs of the various methods.

4.1 Profile Method

Under the general term profile method, all approaches are combined which are based on the flux-gradient similarity (see Sect. 2.3). Because of the progress of the eddy-covariance measurement technique (see Sect. 4.2), the profile method with measurements at several heights has become increasingly irrelevant in the last 10–15 years. The disturbing influence of internal boundary layers makes this technique only applicable in homogeneous terrain with a large uniform fetch. Nevertheless, simple approaches with measurements at only two levels are common; analogue to many parameterization schemes used in atmospheric models.

T. Foken, *Micrometeorology*, DOI 10.1007/978-3-642-25440-6_4

4.1.1 Profile Method with Two Measurement Heights

4.1.1.1 Bulk Approaches

The most simple profile method to determine the energy exchange is the bulk approach, which is also used in models as a zero order closure approach. Bulk approach means that a uniform (linear) gradient is assumed for the given layer and only values at the upper and lower boundaries are used (Mahrt 1996). If the lower boundary of this layer is identical to the surface, than the method is strictly speaking only applicable over water bodies, because only there the gradient between surface values and measurement data at a certain measurement height (mostly 10 m) can be explicitly determined. For instance, the surface temperature and moisture for land surfaces cannot be determined exactly because of roughness elements (plant cover and others). Nevertheless, the method is partly applied by the calculation of surface information measured with satellites, even when considerable losses in the accuracy must be accepted. It is also possible to fix the lowest level at a certain distance above the surface. As a general rule, this should be double the canopy height.

The application of the actual bulk method above water bodies is not without problems, because normally it is not the water surface temperature that is measured but rather the temperature some decimetres below the water surface. Because of the cold film at the surface caused by evaporative cooling, this temperature is about 0.5 K lower than the temperature at the measurement level. The absolute accuracy of the determination of the surface temperature with remote sensing methods is of the same order. Instead of the turbulent diffusion coefficients, bulk coefficients are used. Then the friction velocity can be determined with the drag coefficient C_D and the wind velocity

$$u_* = \sqrt{C_D(z)}\, u(z), \tag{4.1}$$

where it is assumed that the wind velocity at the ground surface is zero.

The sensible heat flux is parameterized with the Stanton number C_H and the latent heat flux with the Dalton number C_E:

$$\frac{Q_H}{\rho\, c_p} = C_H(z)\, u(z)[T(z) - T(0)], \tag{4.2}$$

$$\frac{Q_E}{\rho\, \lambda_p} = C_E(z)\, u(z)[e(z) - e(0)] \tag{4.3}$$

The bulk coefficients are stability and wind velocity dependent. Over the ocean with mostly neutral stratification, the first sensitivity is not a problem. Over the land, the application for non-neutral stratification should be limited to the dynamical sublayer because the bulk coefficients have a remarkable dependency on stratification with differences up to 50% (Brocks and Krügermeyer 1970; Panin

Table 4.1 Coefficients for the determination of the drag coefficient above water bodies according to Eq. (4.4) for $u_{10} < 20$ m s^{-1}

Author	a	b	c in m s^{-1}	u_{10} in m s^{-1}
Foken (1990)	1.2	0	0	<7
	1.2	0.065	7	≥7
Garratt (1992)	1.0	0	0	<3.5
	0.75	0.067	0	≥3.5

1983; Foken 1990). In the literature, a number of relations for the drag coefficient are given (Smith et al. 1996; Geernaert 1999). Currently, the parameterization dependent on the wind velocity at the 10 m reference level is the most useful version. Mean coefficients from a large number of experiments are given in Table 4.1 for the following equation:

$$C_{D10} = [a + b[u_{10} - c]] \cdot 10^{-3} \tag{4.4}$$

For greater wind velocities, the bulk coefficients increase dramatically, and are no longer clearly determined because energy fluxes are much higher under storm conditions than under normal conditions. The values over lakes are slightly higher and over land, where nearly no data are available, they are at least one order of magnitude higher than over the ocean.

The Stanton and Dalton numbers over water are about 20% lower than the drag coefficient. For the same wind velocity classes as given in Table 4.1, the coefficients for Eq. (4.4) have the values $a = 1.0$, $b = 0.054$, $c = 7$ m s^{-1} according to Foken (1990). With increasing roughness the differences compared to the drag coefficient increase (Garratt 1992).

By comparison of Eq. (4.1) with the profile equation for neutral stratification, the relation between the drag coefficient and the roughness height follows as:

$$C_D = \frac{\kappa^2}{\left[\ln\left(\frac{z}{z_0}\right)\right]^2} \tag{4.5}$$

For the determination of the Stanton number, the roughness length for temperature must be considered (for the Dalton number use the roughness length for specific humidity):

$$C_H = \frac{(\kappa/Pr_t)^2}{ln\left(\frac{z}{z_0}\right) ln\left(\frac{z}{z_{0T}}\right)} \tag{4.6}$$

In a similar way, the stability dependence of the bulk coefficients can be determined. Note that slight errors in the determination of the roughness length have a remarkable influence on the bulk coefficients. Therefore, these bulk coefficients are not really an alternative to experimental parameterizations.

Table 4.2 Evaluation of the bulk method

Criterion	Evaluation
Area of application	Application over water, modelling, if no other possibilities
Financial expense	1–3 k€ per system
Personal expense	Low technical maintenance
Education	Introduction
Error	According to the micrometeorological conditions 10–50%
Sampling	1–10 s
Time resolution of fluxes	10–30 min, higher accuracy for daily averages
Application for chemical compounds	For selected inert gases possible
Restrictions in the application	Turbulent conditions necessary

Bulk approaches for the determination of the momentum and energy exchange over water bodies are widely used because the input data are routinely available or can be easily determined, i.e. these data are contained in models. Thus, the roughness parameter is often determined with the Charnock approach, Eq. (2.61).

An overall evaluation, including information about areas of application, cost, and accuracy etc., of the bulk approach is given in Table 4.2. In the following, similar tables are presented for all methods, which allows the reader to easily compare the pros and cons of each approach.

4.1.1.2 Bowen-Ratio Method

The Bowen-ratio method is one of the most common methods used to determine the fluxes of sensible and latent heat. The method is based on Bowen-ratio similarity (see Sect. 2.3.3) and the energy balance equation

$$Bo = \gamma \frac{\Delta \mathrm{T}}{\Delta e}, \tag{4.7}$$

$$-Q_s^* = Q_H + Q_E + Q_G, \tag{4.8}$$

where the psychrometric constant $\gamma = 0.667$ hPa K^{-1} for $p = 1013.25$ hPa and $t = 20$ °C. From both equations, the sensible and latent heat fluxes can be determined:

$$Q_H = (-Q_s^* - Q_G)\frac{Bo}{1 + Bo} \tag{4.9}$$

$$Q_E = \frac{-Q_s^* - Q_G}{1 + Bo} \tag{4.10}$$

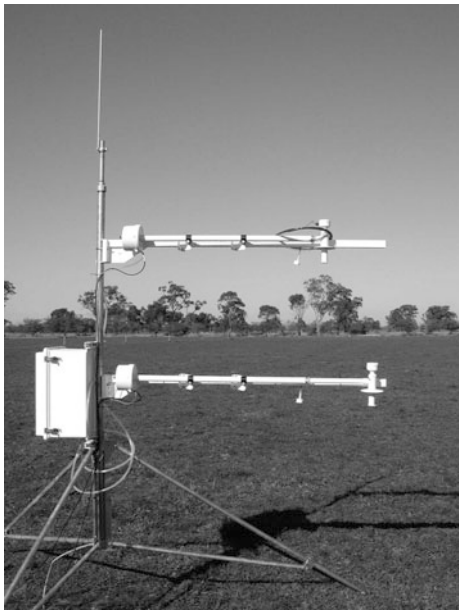

Fig. 4.1 Bowen-ratio measurement system (Published with kind permission of © Campbell Scientific, Inc. Logan UT, USA, All rights reserved)

In addition to net radiation also the ground heat flux, and the temperature and humidity at two levels (see Fig. 4.1) must be determined according to Eq. (4.7).

In addition to the simplifications discussed in Sect. 2.3.4, it is apparent that the equations do not include the wind velocity and do not prescribe a certain difference between the measurement heights. To ensure that a sufficient turbulent regime exists, Foken et al. (1997a) recommend that only measurements with a wind velocity at the upper height greater than 1 m s^{-1} and a difference of the wind velocities between both heights greater than 0.3 m s^{-1} should be used. This requires additional instrumentation with anemometers. Even though the height difference of the measurements (Δz) is not included into the equations, an increase of Δz also increases the difference of the temperature and the humidity. Consequently the influence of the measurement errors decreases. It is therefore recommended to choose a ratio of the measurement heights greater than 4–8 (Foken et al. 1997a). In practice, these requirements are rarely taken into account because measurements over high vegetation have ratios of the aerodynamical heights of about 1.5 (Bernhofer 1992; Barr et al. 1994.). Equations (4.9) and (4.10) are singular for $Bo = -1$. Consequently, unrealistic energy fluxes are predicted for the morning and evening hours. Therefore, the range $-1.25 < Bo < -0.75$ should be excluded from further analysis. To determine the correct sign of the fluxes in the case $Bo < 0$ the following decision criteria are necessary (Ohmura 1982):

$$\begin{aligned} &\text{If} \quad (-Q_s^* - Q_G) > 0 \quad \text{then} \quad (\lambda\Delta q + c_p\Delta T) > 0. \\ &\text{If} \quad (-Q_s^* - Q_G) < 0 \quad \text{then} \quad (\lambda\Delta q + c_p\Delta T) < 0. \end{aligned} \tag{4.11}$$

If these criteria are not fulfilled, the fluxes must be deleted.

The crucial disadvantage of the Bowen-ratio method is that because of the apparent unclosed energy balance (see Sect. 3.8) the residual is either added to the net radiation or distributed according to the Bowen ratio to the sensible and latent heat flux. In general, the fluxes determined with the Bowen-ratio method are larger than those determined with the eddy-covariance method. By definition, the Bowen ratio method fulfils the energy balance equation, but the quantitative accuracy of the fluxes may be limited.

Error analyses for the Bowen-ratio method are widely available (Fuchs and Tanner 1970; Sinclair et al. 1975; Foken et al. 1997a, and references therein). Many of these investigations are based on either single measurements or false assumptions. Often, only the electrical error of the sensor is used (about 0.01–0.001 K), but not the error in the adaptation of the sensor to the surrounding medium and atmosphere with radiation, ventilation and other influences. Only with much effort in measurement techniques is it possible that sensors under the same meteorological conditions and mounted close together show differences as low as 0.05–0.1 K or hPa. Therefore, the errors in temperature and humidity measurements in the atmosphere are significantly higher than the pure electrical error (Dugas et al. 1991).

The error plots given in Fig. 4.5 are taken from Foken et al. (1997a), and are based on an accepted measurement error of ±0.05 K or hPa. From Fig. 4.2 we see that a 20 and 40% error in the Bowen ratio corresponds to about a 10 and 20% error

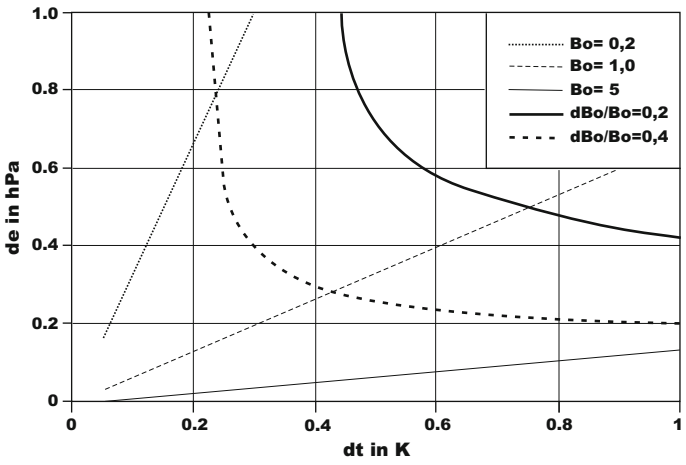

Fig. 4.2 Error of the Bowen ratio (20 und 40%) dependent on the measured temperature and water vapour differences (Adapted from Foken et al. 1997a, with kind permission of © Austrian Meteorological Society, Vienna 1997, All rights reserved)

Table 4.3 Evaluation of the Bowen-ratio method

Criterion	Evaluation
Area of application	Applied research, partly continuously running programs
Financial expense	10–15 k€ per system
Personal expense	Continuous scientific and technical support
Education	Knowledge in micrometeorology and measurement technique
Error	According to the micrometeorological conditions 10–30% (assumption of a closed energy balance)
Sampling	1–10 s
Time resolution of fluxes	10–30 min
Application for chemical compounds	For selected inert gases possible
Restrictions in the application	Sufficient footprint area, turbulent conditions necessary

in the sensible and latent heat flux respectively. Consideration of the three values of Bowen ratios in Fig. 4.5 shows that optimal conditions exist for $Bo = 0.677$ and the Bowen ratio should not significantly differ from this value. To realize errors of <20% (<40%) for the Bowen ratio, the temperature and humidity differences must be >0.6 (>0.4) K or hPa. This underlines the requirement for large differences in the measurement heights. Limitations result from internal boundary layers and possible roughness sublayers, which should be avoided within the measurement range. Note that in this error analysis, possible errors due to energy imbalance were not taken into account.

An overall evaluation of the method is given in Table 4.3. The evaluations of the errors of the method are based on the assumption of accurate net radiometer measurements (see Sect. 6.2.1), which require sensors costing at least 4 k€. Furthermore, the heat storage in the soil should be calculated very accurately to reduce the influence of the residual of the energy balance closure.

4.1.1.3 Modified Bowen-Ratio Method

According to Businger (1986), the modified Bowen-ratio method (see Eq. 2.89) is based on the application of Bowen-ratio similarity (see Sect. 2.3.4) and does not use the energy balance equation, i.e. it avoids the related energy balance closure issues (see Sect. 3.8). The method benefits both from the Bowen-ratio similarity (Eq. 2.99) and also from direct measurements of the buoyancy flux with a sonic anemometer according to the eddy-covariance method (see Sect. 4.2), which can be re-calculated into the sensible heat flux (Schotanus et al. 1983; Liu et al. 2001). Such a measurement system is shown in Fig. 4.3 (Liu and Foken 2001). Usual limitations of the Bowen-ratio method are not valid when the modified Bowen-ratio is used. However, the recommended ratio of the measurement heights of $z_2/z_1 = 4$–8 is still required to reduce the measurement errors. Also, the observed data are not

Fig. 4.3 Measurement system for the modified Bowen-ratio method (METEK GmbH Elmshorn and Th. Friedrichs & Co. Schenefeld near Hamburg; *Photograph* Foken)

useful when the friction velocity $u_* < 0.07$ m s^{-1} and the Bowen ratio $Bo \sim 0$. Because of the decreasing cost of sonic anemometers, they are now in the price range of good net radiation sensors, the overall measurement costs do not increase. Furthermore, the expensive measurements of the soil heat flux and the heat storage in the soil are no longer necessary. The Bowen ratio can be calculated with Eq. (4.7), and the latent heat flux can be calculated with:

$$Q_E = \frac{Q_H}{Bo}. \tag{4.12}$$

The modified Bowen-ratio method was originally developed for the determination of trace gas fluxes (Businger 1986; Müller et al. 1993). According to Eq. (2.99) a turbulent flux, e.g. the sensible heat flux, can be directly determined, and from the relevant difference (here temperature difference, ΔT) and the concentration difference, Δc, between two measurement levels, the trace gas flux (dry deposition) can be calculated using:

$$Q_c = Q_H \frac{\Delta_c}{\Delta T} \tag{4.13}$$

Table 4.4 Evaluation of the modified Bowen-ratio method

Criterion	Evaluation
Area of application	Applied research, partly continuously running programs
Financial expense	10–15 k€ per system
Personal expense	Continuous scientific and technical support
Education	Knowledge in micrometeorology and measurement technique
Error	According to the micrometeorological conditions 10–30%
Sampling	1–10 s, 10–20 Hz for turbulent flux
Time resolution of fluxes	10–30 min
Application for chemical compounds	For selected inert gases possible
Restrictions in the application	Sufficient footprint area, turbulent conditions necessary, similarity of the turbulence characteristics necessary

In an analogues way to the Bowen-ratio method, criteria for and limitations of the method, which are dependent on the deposited or emitted matter, must be developed. The wind or friction velocity criteria can be used; also, the turbulent scales of both scalars must be similar (see Sects. 2.5 and 4.4). An overall evaluation of the methods is given in Table 4.4.

4.1.1.4 Further Parameterization Methods

The determination of turbulent fluxes with observations at only two heights is an interesting measurement approach because the fluxes can be estimated in a simple way. While the bulk method requires a uniform (linear) gradient between both measurement heights and the Bowen-ratio method requires similar gradients of both parameters, there is also the possible solution of the profile equations with stability influences (Eqs. 2.74–2.76) for two heights. Corresponding proposals (Itier 1980; Lege 1981) were used by Richter and Skeib (1984) for a method to determine the turbulent fluxes in an iterative way. They introduced a critical height, z_c, which is approximately equal to the height of the dynamical sublayer. Below this height, the equations for neutral stratification can be applied. The use of the universal functions by Skeib (1980), which allows for this method a simple layer-wise integration, gives the following equations for the flux calculation (Richter and Skeib 1991):

$$u(z_2) - u(z_1) = \frac{u_*}{\kappa} \begin{Bmatrix} \ln\left(\frac{z_2}{z_1}\right) & z_1 < z_2 < z_c \\ \ln\left(\frac{z_c}{z_1}\right) + \frac{1}{n_u}\left[1 - \left(\frac{z_2}{z_c}\right)^{-n_u}\right] & z_1 \le z_c \le z_2 \\ \frac{1}{n_u}\left[\left(\frac{z_1}{z_c}\right)^{-n_u} - \left(\frac{z_2}{z_c}\right)^{-n_u}\right] & z_c < z_1 < z_2 \end{Bmatrix} \tag{4.14}$$

In an analogues way, follow the equation for the sensible and latent heat flux:

Table 4.5 Coefficients for Eqs. (4.14) and (4.15)

Stability range	$\varsigma < 0$	$\varsigma > 0$
ς_c	−0.0625	0.125
n_u	0.25	−1
n_T	0.5	−2

Table 4.6 Weighting factor R for Eq. (4.16) according to Richter and Skeib (1984)

z_2/z_1	2	4	8	16
$-0.0625 \leq \varsigma \leq 0.125$	0.693	0.462	0.297	0.185
$-1 < \varsigma < -0.0625$	0.691	0.456	0.290	0.178
$0.125 < \varsigma < 1$	0.667	0.400	0.222	0.118

$$T(z_2) - T(z_1) = \mathrm{Pr}_t \frac{\overline{w'T'}}{\kappa\, u_*} \begin{Bmatrix} \ln\left(\frac{z_2}{z_1}\right) & z_1 < z_2 < z_c \\ \ln\left(\frac{z_c}{z_1}\right) + \frac{1}{n_T}\left[1 - \left(\frac{z_2}{z_c}\right)^{-n_T}\right] & z_1 \leq z_c \leq z_2 \\ \frac{1}{n_T}\left[\left(\frac{z_1}{z_c}\right)^{-n_T} - \left(\frac{z_2}{z_c}\right)^{-n_T}\right] & z_c < z_1 < z_2 \end{Bmatrix} \tag{4.15}$$

The coefficients in Eqs. (4.14) and (4.15) are given in Table 4.5. The critical height, which is a function of the bulk-Richardson number (Eq. 2.83) and a weighting factor R (the stability-dependent curvature of the profile according to Table 4.6), is given by:

$$z_c = \frac{\varsigma_c}{\varsigma_1} z_1 = \frac{\varsigma_c}{R\, Ri_B} \tag{4.16}$$

The application of the method requires an iterative solution of the equation. Starting with an initial estimate of ς_c, the friction velocity and then the sensible heat flux are calculated. Using these values, an updated value for ς_c is calculated, and the process is repeated. After about 3–6 iteration steps, the method converges. As a measurement technique the Bowen-ratio system without net radiometer but with anemometers at both measurement heights can be used. The wind velocity criterion of the Bowen-ratio method, which is a test on developed turbulence, must also be applied here. Also, measurements must be excluded when the wind and temperatures differences between the two levels are of the order of the measurement error. The method can be extend in principle by using humidity and/or concentration measurements to measure the latent heat and/or deposition flux. An overall evaluation is given in Table 4.7.

4.1.1.5 Quality Assurance

For all profile measurements with two measurement levels, it should be demonstrated that the measurement accuracy is at least 10-fold greater than the expected difference between the two measurement heights such that the flux can at least be determined with an accuracy of 20% (positive and negative measurement errors are

Table 4.7 Evaluation of the parameterization approach according to Richter and Skeib (1991)

Criterion	Evaluation
Area of application	Applied research, partly continuously running programs
Financial expense	10–15 k€ per system
Personal expense	Continuous scientific and technical support
Education	Knowledge in micrometeorology and measurement technique
Error	According to the micrometeorological conditions 10–30%
Sampling	1–10 s
Time resolution of fluxes	10–30 min
Application for chemical compounds	For selected inert gases possible
Restrictions in the application	Sufficient footprint area, turbulent conditions necessary

assumed). It is further assumed that wind and temperature measurements can be made with a sufficient accuracy. According to a method proposed by Foken (1998), the profile equations Eqs. (2.74)–(2.76) can be divided into a turbulence-related part and in the difference of the state parameter between both heights:

$$Q_c = Q_N[u_*, \varphi(z/L), \ln(z-d)]\Delta_c \tag{4.17}$$

The normalized flux Q_N is plotted in Fig. 4.4. The minimal measurable flux with 20% accuracy is the 10-fold resolution of the measurement system c_{min}:

$$Q_{c,\min} = Q_N 10\, c_{\min} \tag{4.18}$$

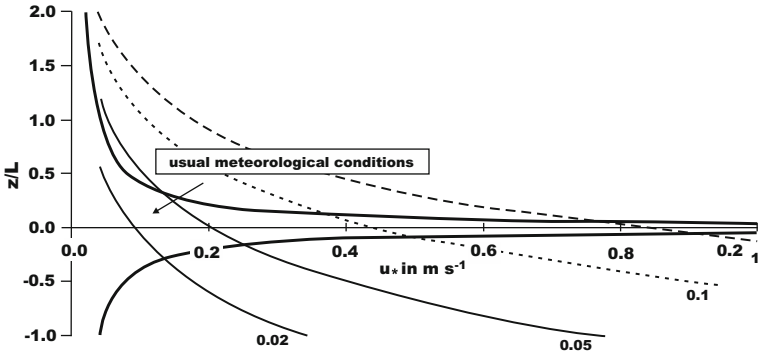

Fig. 4.4 Course of the normalized flux Q_N in dependency of the stratification and the friction velocity for m = z_2/z_1 = 8 (Adapted from Foken 1998, with kind permission of © German Meteorological Service, Offenbach 1998, All rights permitted)

Table 4.8 Minimal determinable flux (20% error) for energy and different matter fluxes above low ($m = z_2/z_1 = 8$) and tall ($m = 1.25$) vegetation for neutral stratification and $u_* = 0.2$ m s^{-1} (units µg m^{-3} for concentrations and µg s^{-1} m^{-2} for fluxes), the italic fluxes are larger than the typical fluxes (Foken 1998, completed)

Energy or matter flux	c_{min}	$\Delta_{c.min}$	Flux m = 8	Flux m = 1.25
Sensible heat	0.05 K	0.5 K	0.025 m K s^{-1} 30 W m^{-2}	0.05 m K s^{-1} 60 W m^{-2}
Latent heat	0.05 hPa	0.5 hPa	0.025 hPa m s^{-1} 45 W m^{-2}	0.05 hPa m s^{-1} 90 W m^{-2}
Nitrate particles	0.01	0.1	0.005	0.01
Ammonium particles	0.02	0.2	0.01	*0.02*
CO_2	100	1000	50	100
NO	0.06	0.6	*0.03*	*0.06*
NO_2	0.1	1.0	0.05	0.1
O_3	1.0	10.0	0.5	*1.0*
NH_3	0.014	0.14	0.007	0.014
HNO_3	0.2	2.0	*0.1*	*0.2*
HNO_2	0.25	2.5	*0.125*	*0.25*

Typical values of minimum measurable fluxes over low and high vegetation are given in Table 4.8.

4.1.2 Profile Measurements with Several Measurement Heights

In Sect. 4.1.1, special cases of the profile method with only two measurement heights were discussed. The classical profile method (Fig. 4.5) is based on wind, temperature and moisture measurements made at 3–6 levels, where 4–6 levels are optimum (Foken and Skeib 1980). These measurements were more widely used about 20 years ago because the eddy-covariance method was too costly. Today, profile measurements are applied most often in basic research to determine parameters of the profile equation or disturbances by internal and stable boundary layers.

The basis for the profile method in the neutral case are Eqs. (2.48)–(2.50) or in the integral form as in Eq. (2.60). The simplest case is the linear approximation, which is more or less also the basis of the bulk and Bowen-ratio method:

$$\left(\frac{\partial X}{dz}\right)_{z_a} \cong \frac{\Delta X}{\Delta z} = \frac{X_2 - X_1}{z_2 - z_1} \qquad z_a = (z_1 - z_2)^{1/2} \tag{4.19}$$

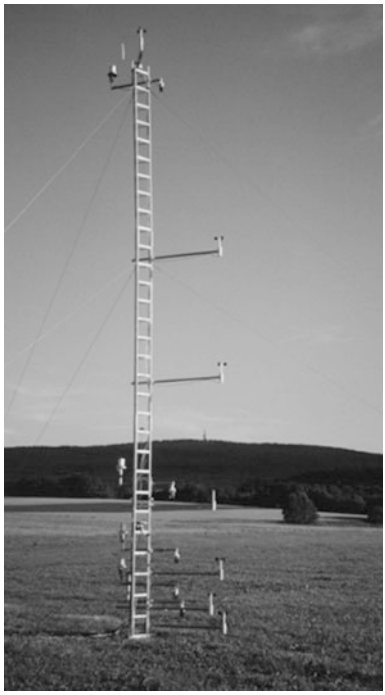

Fig. 4.5 Measurement mast for profile measurements (*Photograph* Foken)

The logarithmic approximation is a much better representation of the physical facts with a geometric average of the heights:

$$\left(\frac{\partial X}{\partial \ln z}\right)_{z_m} \cong \frac{\Delta X}{\Delta \ln z} = \frac{X_2 - X_1}{\ln(z_2/z_1)} \qquad z_m = (z_1\, z_2)^{1/2} \tag{4.20}$$

The basis for the profile method in the diabatic case are Eqs. (2.74)–(2.76). For a simple graphical analysis, the integral form (Eq. 2.86) is used with $\ln z - \psi(z/L)$ on the ordinate and u or T on the abscissa according to the following equations (Arya 2001):

$$\ln z - \psi_m(z/L) = \frac{\kappa}{u_*} u + \ln z_0 \tag{4.21}$$

$$\ln z - \psi_H\left(\frac{z}{L}\right) = \frac{\kappa/Pr_t}{T_*} T - \ln \frac{\kappa/Pr_t}{T_*} T_0 + \ln z_{0T} \tag{4.22}$$

Before both equations can be calculated, either the Richardson number (Eq. 2.82 or 2.83) or the Obukhov length (Eq. 2.72) must be determined. The method can be solved iteratively.

There are approximations that are not directly based on the profile equation. The simplest is the series expansion:

$$u(z) = a_0 + a_1 \ln z + a_2 z \tag{4.23}$$

A more commonly used expansion is one developed by Kader and Perepelkin (1984), which is superior to Eq. (4.23):

$$u(z) = a_0 + \frac{a_1 \ln z + a_3 + a_4 z^{2/3}}{5 + z} \tag{4.24}$$

For the interpolation of profiles, several approaches are used, for example, spline methods. To insure that these methods do not overcorrect measurement errors and falsify the result, special cubic interpolation methods between neighbouring grid points should be used (see e.g. Akima 1970).

Because of the availability of powerful personal computers, lavish interpolation methods are used such as the Nieuwstadt-Marquardt approach. In this approach, a quadratic cost function is calculated as a measure of the tolerance between the measured data and the model based on the profile equations (Nieuwstadt 1978). The nonlinear system of equations to minimize the cost function can be solved using the method described by Marquardt (1983).

As with the Bowen ratio method, the profile method requires high accuracies in the measurements. High ratios of the upper to the lower measurement height, and negligible influences from the surface are also necessary. The wind criteria for the Bowen ratio method to exclude non-turbulent cases can be also used. A complete error analysis was made by Foken and Skeib (1980). An overall evaluation is given in Table 4.9.

Table 4.9 Overall evaluation of the profile method with 4–6 measurement heights

Criterion	Evaluation
Area of application	Basic and applied research, partly continuously running programs
Financial expense	10–15 k€ per system
Personal expense	Continuous scientific and technical support
Education	Good knowledge in micrometeorology and measurement technique
Error	According to the micrometeorological conditions 5–20%
Sampling	1–10 s
Time resolution of fluxes	10–30 min
Application for chemical compounds	For selected inert gases possible
Restrictions in the application	Sufficient footprint area, turbulent conditions necessary

4.1.3 Power-Law

For many applied methods, the power-law is widely used for the determination of the wind distribution near the ground surface. Such power-law expressions approximately agree only with respect to shape with the physical equations given in Sect. 2.3. They are not only applied in the surface layer but also in the lower part of the atmospheric boundary layer (Doran and Verholek 1978; Sedefian 1980; Joffre 1984; Wieringa 1989; Hsu et al. 1994):

$$\frac{u_1}{u_2} = \left(\frac{z_1}{z_2}\right)^p \tag{4.25}$$

For wind power applications, an exponent of $p = {}^1/_7$ is often applied (Peterson and Hennessey 1978). Detailed approaches use a stability and roughness dependency on the exponent. After differentiation of Eq. (4.25), it follows according to Huang (1979):

$$p = \frac{z}{u}\frac{\partial u}{\partial z} \tag{4.26}$$

This version allows complicated approaches including the roughness of the surface and the stratification expressed with universal functions. Irvin (1978) proposed the approach

$$p = \frac{u_*}{u\,\kappa}\varphi_m(\varsigma). \tag{4.27}$$

Similar is the approach by Sedefian (1980):

$$p = \frac{\varphi_m\left(\frac{\bar{z}}{L}\right)}{\left[\ln\left(\frac{\bar{z}}{z_0}\right) - \psi_m\left(\frac{\bar{z}}{L}\right)\right]} \tag{4.28}$$

Huang (1979) used this form of the exponent with the universal function given by Webb (1970) and Dyer (1974) and a special integration for large roughness elements. For unstable stratification, it follows that

$$\begin{aligned} p &= \frac{\left(1 - 19.3\frac{z}{L}\right)^{-1/4}}{\ln\frac{(\eta-1)(\eta_0+1)}{(\eta+1)(\eta_0-1)} + 2\tan^{-1}\eta - 2\tan^{-1}\eta_0} \\ \eta &= \left(1 - 19.3\frac{z}{L}\right)^{1/4} \quad \eta_0 = \left(1 - 19.3\frac{z_0}{L}\right)^{1/4} \end{aligned} \tag{4.29}$$

and for stable stratification:

$$p = \frac{1 + 6\frac{z}{L}}{\ln\frac{z}{z_0} + 6\frac{z}{L}} \tag{4.30}$$

The numbers in both equations differ from those in the original reference according to the investigations by Högström (1988). This approach is for instance used in the footprint model by Kormann and Meixner (2001).

The application of this method is not without problems. In the morning daylight hours, these approaches are in a good agreement with measurements, but in the early afternoon—with the start of the thermal internal boundary layer (see Sect. 3.2.3)—the values of the stratification measured in the surface layer cannot be applied to the whole profile. An overall evaluation of the method is given in Table 4.10.

An interesting approach was given with the definition of the radix layer (Santoso and Stull 1998), which is approximately one fifth of the atmospheric boundary layer (surface layer and lower part of the upper layer). In the uniform layer above the radix layer, no increase of the wind velocity occurs and a constant wind velocity u_{RS} predominates:

$$\frac{u(z)}{u_{RS}} = \begin{cases} \left(\frac{z}{z_{RS}}\right)^A \exp\left[A\left(1 - \frac{z}{z_{RS}}\right)\right] & z \le z_{Rs} \\ 1 & z > z_{Rs} \end{cases} \tag{4.61}$$

Until now, the radix-layer method has been rarely used and it is limited to convective conditions. Furthermore there are difficulties to determine the height z_{RS} of the radix layer.

Table 4.10 Evaluation of exponential approaches for the determination of the wind profile in the lowest 100 m

Criterion	Evaluation
Area of application	Engineer-technical applications, continuously running programs
Financial expense	1–3 k€ per system
Personal expense	Continuous technical support
Education	Experiences in measurement technique
Error	According to the micrometeorological conditions 5–20% (unstable stratification), otherwise significant larger errors
Sampling	1–5 s
Time resolution of the gradients	10–30 min
Restrictions in the application	Only for unstable stratification sufficient accuracy, significant influences by internal boundary layers, band thermal internal boundary layers at the afternoon for near surface measurements, turbulent conditions necessary

4.2 Eddy-Covariance Method

4.2.1 General Basics

Flux measurements using the eddy-covariance method (often also called eddy-correlation method, but this can bring some confusions, see Sect. 4.3) are a direct measurement method without any applications of empirical constants (Haugen 1973; Businger 1986; Kaimal and Finnigan 1994; Foken et al. 1995, 2012b Lee et al. 2004; Aubinet et al. 2012a). However, the derivation of the mathematical algorithm is based on a number of simplifications so that the method can be applied only if these assumptions are exactly fulfilled (see Sect. 2.1.2). The quality of the measurements primarily depends more on the on-site conditions and the application of necessary corrections than on the presently available highly sophisticated measurement systems. Therefore experimental experience and knowledge of the special character of atmospheric turbulence have a high relevance. The most limiting conditions are the assumptions of horizontally homogeneous surfaces and steady-state conditions. The exact determination of the footprint area (see Sect. 3.4), which should be over a uniform underlying surface for all stability conditions, and the exclusion of internal boundary layers and obstacle influences (see Sects. 3.2 and 3.3) are critical for the selection of the measurement site. This is especially relevant for forest sites, where additional specifics of tall vegetation must be taken into account (see Sect. 3.5).

The basic equations are comparatively simple (see Eqs. 2.23 and 2.24):

$$u_*^2 = \overline{-u'w'},\ \frac{Q_H}{\rho\, c_p} = \overline{T'w'},\ \frac{Q_E}{\rho\, \lambda} = \overline{q'w'},\ \frac{Q_c}{\rho} = \overline{c'w'} \tag{4.32}$$

The covariance of the vertical wind velocity, w, and either one of the horizontal wind components or of a scalar x can be determined in the following way:

$$\begin{aligned} \overline{w'x'} &= \frac{1}{N-1}\sum_{k=0}^{N-1}\left[(w_k - \overline{w_k})(x_k - \overline{x_k})\right] \\ &= \frac{1}{N-1}\left[\sum_{k=0}^{N-1} w_k\, x_k - \frac{1}{N}\left(\sum_{k=0}^{N-1} w_k \sum_{k=0}^{N-1} x_k\right)\right] \end{aligned} \tag{4.33}$$

Since the method is not applied directly at the surface but at a certain height above the surface and partially also above heterogeneous terrain, further assumption must be made. Figure 3.30 schematically illustrates for flat and sloped terrain that in addition to the vertical flux at the upper boundary of a volume element horizontal and vertical fluxes through the volume exist, which in the simplest case balance each other. For flat terrain the net flux of a scalar is:

$$F_\chi = \underbrace{\overline{\rho_d}\,\overline{w'\chi'}\big|_h}_{I} + \underbrace{\int_0^{z_m} \overline{\rho_d}\,\frac{\overline{\partial\chi}}{\partial t}\,dz}_{II} \tag{4.34}$$

The term II is the source or sink term between the surface and the measurement height, which can be ignored for the momentum and sensible heat or buoyancy flux. In most cases, it is also negligible for the latent heat flux. However, for other gases, like carbon dioxide, its contribution can be significant. In particular, in the morning hours, when the storage near the ground disappears, the source term is important. Term I is the ***flux at the upper boundary of the volume element measured with the eddy-covariance method***.

In heterogeneous terrain, the net flux is the flux at the upper boundary of the volume element (term I), the source and sink term II (calculated from the change in time of the partial density of the investigated matter), and also a horizontal (term III) and vertical (term IV) advection term (see Eq. 3.33) must be taken into account:

$$F_\chi = \underbrace{\overline{\rho_d}\,\overline{w'\chi'}\big|_h}_{I} + \underbrace{\int_0^{z_m} \overline{\rho_d}\,\frac{\overline{\partial\chi}}{\partial t}\,dz}_{II} + \underbrace{\int_0^{z_m} \left[\overline{\rho_d u}\,\frac{\overline{\partial\chi_x}}{\partial x} + \overline{\rho_d v}\,\frac{\partial\overline{\chi_y}}{\partial y}\right]}_{III} + \underbrace{\int_0^{z_m} \left[\overline{\rho_d w}\,\frac{\partial\overline{\chi}}{\partial z}\right]}_{IV} \tag{4.35}$$

The advection term of the fluxes was neglected, because it is obviously very small and it cannot be measured with a sufficient accuracy. In this form the method is called ***Generalized Eddy-Covariance Method***.

Lee (1998) showed that term IV should also include the change of the vertical velocity, $\int_0^{z_m}\left[\overline{\rho_d w}\frac{\partial\overline{\chi}}{\partial x} + \overline{\rho_d \chi}\frac{\partial\overline{w}}{\partial z}\right]$. In the discussion of this paper, Paw U et al. (2000) concluded that the change of the vertical velocity is already part of the WPL-correction (Webb et al. 1980), which further includes the vertical advection term discussed by Lee (1998). However, it is required that the coordinate system follows the stream lines after a coordinate transformation (see Sect. 4.2.3).

Especially in complex terrain, the advection problem is still subject of ongoing research efforts and expensive experiments (Aubinet et al. 2003a, 2005, see Sect. 3.6). Due to the large errors in the determination of the advection terms it is recommended that no corrections are applied at sites without obvious indication of advection being an important factor (Aubinet et al. 2010). Instead it is recommended to exclude data sets collected at night under low-turbulence conditions. In such cases, the fluxes should be parameterized (see Sect. 4.2.6, Aubinet et al. 2012b).

4.2.2 Basics in Measurement Technique

According to Eq. (4.32), the turbulent fluctuations of the components of the wind vector and of scalar parameters must be measured at a high sampling frequency (see Sect. 6.1.2) so that the turbulence spectra (see Sect. 2.5) can be extended to 10–20 Hz. The measurement devices used for such purposes are sonic anemometers for the wind components and sensors that can measure scalars with the required high resolution in time. The latter are often optical measurement methods (see Sect. 6.2.3). The measurement or sampling time depends on the atmospheric stratification, the wind velocity, and the measurement height. For heights of 2–5 m, 10–20 min would be required for daytime unstable stratification (summer) and about 30–60 and sometimes as high as 120 min for nighttime stable stratification. The measurement errors are not significant if a sampling time of 30 min is used over the entire day. For short sampling times, the low frequency contributions to the fluxes are missed, and for long sampling times the steady state condition may not be fulfilled. Accordingly, the flux can be determined only after the measurements have been made. It is also possible to use filtering options. Low pass filters or trend eliminations can create errors in the fluxes, (Rannik and Vesala 1999; Finnigan et al. 2003), thus block averaging with an averaging time of 30 min is now recommended. Due to the spectral character of turbulence, fluxes are measured only partially if only short averaging intervals are available (5–10 min). The simple summation over longer time periods is incorrect. Special correction algorithms are necessary, and these need further statistical parameters of the short time periods. For the covariance of a long time series of M data points, based on N short-time series each with U data points, where $N = M/U$, it follows (Foken et al. 1997b, method was proposed by G. Peters):

$$\overline{w'x'} = \frac{1}{M-1}\left[(U-1)\sum_{j=1}^{N}\left(\overline{w'x'}\right)_j + U\sum_{j=1}^{N}\overline{w_j}\,\overline{x_j} - \frac{U^2}{M}\sum_{j=1}^{N}\overline{w_j}\sum_{j=1}^{N}\overline{x_j}\right] \tag{4.36}$$

The height of the measurements depends on the path length and the separation between a sonic anemometer and an additional device (e.g. hygrometer). Devices with a path length less than 12 cm should not be used below 2 m, and devices with a path length more than 20 cm should not be used below 4 m. The minimum distance between a sonic anemometer and an additional device, depends on the flow distortions caused by the devices and should be determined in a wind tunnel. Typically, for fine-wire temperature sensors, the minimum distance is 5 cm, and for hygrometers it is 20–30 cm. These additional instruments should be mounted downwind of the sonic anemometers and 5–10 cm below the wind measurement path (Kristensen et al. 1997). Therefore, to reduce the corrections of the whole system (see Sect. 4.2.3) the measurement height must be estimated not only dependent on the path length of the sonic anemometer but also dependent on the separation of the measurement devices. Also, the measurement height should be twice the canopy height in order to exclude effects of the roughness sublayer. Flow distortions due to the measurement system can hardly be avoided (Dyer 1981),

Fig. 4.6 Eddy-covariance measurement complex of the University of Bayreuth with a sonic anemometer CSAT3, IR-hygrometer LiCor 7500, and hygrometer KH20 in the back ground (*Photograph* Foken)

however corrections with coordinate rotations are possible (Sect. 4.2.3). Nevertheless, care must be taken that instrument mounts, tower elements, or other sensors are installed at a sufficient distance to the turbulence measurements (distance 5–10fold of the dimension, Wieringa 1980; Wyngaard 1981; Wyngaard et al. 1982; Barthlott and Fiedler 2003).

In basic research, sonic anemometers (Fig. 4.6, see Sect. 6.2.2) with a selected inflow sector to exclude flow distortion are used. For most applications, wind direction-independent omni-directional sonic anemometers are sufficient, but these have flow distortions due to mountings and sensor heads. For flux measurements, it is important that interfering parts of devices are kept at a minimum, in particular below the measurement path for the vertical component of the wind, because the vertical oscillations of relatively small turbulence elements are much faster than the horizontal movements of larger turbulence elements. This difference can be noted in the frequency shift of the spectral maximum for vertical and horizontal wind fluctuations by more than one order (see Sect. 2.5).

Most of the sonic anemometers also measure the fluctuations of the sound velocity and therefore indicate the so-called sonic temperature (nearly identical with the virtual temperature). The flux calculated with this temperature is the buoyancy flux, about 10–20% greater than the sensible heat flux:

$$\frac{Q_{HB}}{\rho c_p} = \overline{w' T_v'} \tag{4.37}$$

The sensible heat flux can be determined by applying additional corrections, which need additional moisture measurements (see Sect. 4.2.3.5). More expensive are direct temperature measurements made with thin thermocouples or free spanned resistance wires (diameter <15 µm to reduce the radiation error, see Sect. 6.2.3.2).

Hygrometers are used for the determination of the latent heat flux (evaporation). Such devices are nowadays mostly optical devices. These have either an open path or are a closed path. The open path hygrometer is mounted near the sonic anemometer, and the closed path is mounted some meters away and the air is aspirated below the sonic anemometer. The first works in the UV and IR range, and the second works only in the IR range. UV devices should be used for low humidity conditions (water vapour pressure 0–20 hPa) and IR devices for high moistures (10–40 hPa). Closed path devices need extensive data corrections. One correction accounts for the time delay of the measurement signal in relation to the wind measurements, and another correction accounts for the filtering of the fluctuations by the tube (Leuning and Judd 1996; Aubinet et al. 2000; Ibrom et al. 2007a, b). These devices have the benefit of directly measuring the mixing ratio, while open-path devices measure the absolute concentration and need a density correction (WPL-correction, see Sect. 4.2.3.6). The effort for maintenance and calibration for all devices is considerable. The lifetime of UV devices is very limited (<1000 h). Very fast optical devices for other gaseous components (e.g. ozone, nitrogen oxide, sulphur dioxide) are also available and the deposition flux can be measured in a similar way. Nowadays increasingly tuneable lasers are applied (Bowling et al. 2003; Pattey et al. 2006), which are commercially available for carbon dioxide, carbon isotopes 12 and 13, methane, nitrous oxide, and other gases.

Recently, extensive software packages for the analysis of eddy-covariance measurements have become available, mostly free of charge, from universities, institutions and commercial companies (Appendix A.7). They differ in their application for users without extensive knowledge of the methods and researches, who need a high variability in the data analysis. Comparison studies, which are available for most of the programs, have shown that software packages can be reliably applied (Mauder et al. 2008; Fratini and Mauder 2014). Nevertheless, they differ slightly in the applications of correction and quality control methods. Therefore, the user needs some basic knowledge about these methods. Based on recent knowledge, versions of the software developed by McMillen (1988), which includes an internal rotation of the coordinates with a moving average, should no longer be applied. Furthermore, only well documented software packages should be used.

4.2.3 Applicable Correction Methods

The eddy-covariance method is based on a number of assumptions (see Sect. 2.1.2), and if these assumptions are not met, corrections must be applied to the collected data. However, it is often not clear which corrections are necessary. The data are thus screened with extensive tests (see Sect. 4.2.5), primarily after all corrections

are applied to the data. Important are the tests for steady-state conditions and developed turbulence.

4.2.3.1 Control of the Raw Data

The application of correction methods is closely connected with the data quality control (see Sects. 4.2.5 and 6.3). It starts with the exclusion of missing values and outliers, which can be found by electrical and meteorological plausibility tests.

Further tests should detect unfavourable meteorological conditions or technical problems of the instruments, whereby separating these two factors is often difficult (Vickers and Mahrt 1997). Spikes, i.e. values that are significantly above the normal measurement value but still within the possible range, are often electronically caused. The usual test is the determination of the standard deviation. All values greater than 3.5σ (Højstrup 1993) are considered as spikes. If single spikes are large, it is recommended to repeat the test 2–3 times, because otherwise erroneous data cannot be identified. Measurement series with more than 1% of spikes should not be used. More robust is the application of the absolute deviation from the median (MAD, Hoaglin et al. 2000), $MAD = median_i\left(\left|x_i - median_j\left(x_j\right)\right|\right)$, where all values are identified as spikes, which are larger or lower than a multiple of the MAD-value

$$median(x) - \frac{q\ MAD}{0.6745} \leq x_i \leq \frac{q\ MAD}{0.6745} + median(x), \tag{4.38}$$

where 0.6745 is the corresponding value of the normal distribution by Gauß. It is recommended to use $q = 7$ for this application (Mauder et al. 2013).

If the same data logger records several measurement signals, it may occur that the data measured at the same point of time are not stored at the same point of time. This can be partially corrected in the software of the data logger, but such time delays can change with time. A typical example is a measurement system where a gas is aspirated with a tube at the sonic anemometer. Then, depending on the flow velocity within the tube, concentration measurements can be recorded significantly later than the wind component. A cross-correlation analysis is recommended and the concentration time series are shifted relative to the vertical wind measurements by the time difference of maximum cross-correlation. This must be done before any further calculations are made.

After the time shift is applied, initial covariances can be calculated. It is helpful to store these, because the first two steps use most of the calculation time. The next step is the rotation of the coordinates. In research studies, the *planar-fit* method (Wilczak et al. 2001) is currently most often used. This rotation method is applied to the data over the entire measurement campaign. Therefore, only preliminary results are available up to the end of the experiment.

The following corrections are given in the order of their application. Because some quantities, such as the stability parameter, must be calculated from the

corrected data, but are also used in the correction algorithms, their values should be updated iteratively. The iterations often converge after a few cycles, leading to an improvement of the fluxes by 1% (Mauder et al. 2006).

4.2.3.2 Coordinate Rotation (Tilt Correction)

A basic condition for applying the eddy-covariance method is the assumption of a negligible mean vertical wind component (see Eq. 2.5). Otherwise advective fluxes must be corrected (see Sect. 3.6). This correction is called tilt correction and includes the rotation of a horizontal axis into the mean wind direction. It is based on works by Tanner and Thurtell (1969) and Hyson et al. (1977). The first correction is the rotation of the coordinate system around the z-axis into the mean wind. Using the measured wind components (subscript m), the new components are given by (Kaimal and Finnigan 1994)

$$\begin{aligned} u_1 &= u_m \cos\theta + v_m \sin\theta, \\ v_1 &= -u_m \sin\theta + v_m \cos\theta, \\ w_1 &= w_m, \end{aligned} \tag{4.39}$$

where

$$\theta = \tan^{-1}\left(\frac{\overline{v_m}}{\overline{u_m}}\right). \tag{4.40}$$

For an exact orientation of the anemometer into the mean wind and for small fluctuations of the wind direction (<30°), this rotation is not necessary (Foken 1990). The friction velocity can be calculated from the horizontal wind component orientated into the mean wind direction; otherwise Eq. (2.26) must be applied. With today's high computer power, this special case has little significance.

The second rotation is around the new y-axis until the mean vertical wind disappears (Kaimal and Finnigan 1994)

$$\begin{aligned} u_2 &= u_1 \cos\phi + w_1 \sin\phi \\ v_2 &= v_1, \\ w_2 &= -u_1 \sin\phi + w_1 \cos\phi, \end{aligned} \tag{4.41}$$

where

$$\phi = \tan^{-1}\left(\frac{\overline{w_1}}{\overline{u_1}}\right). \tag{4.42}$$

Both rotations are graphically shown in Fig. 4.7a, above.

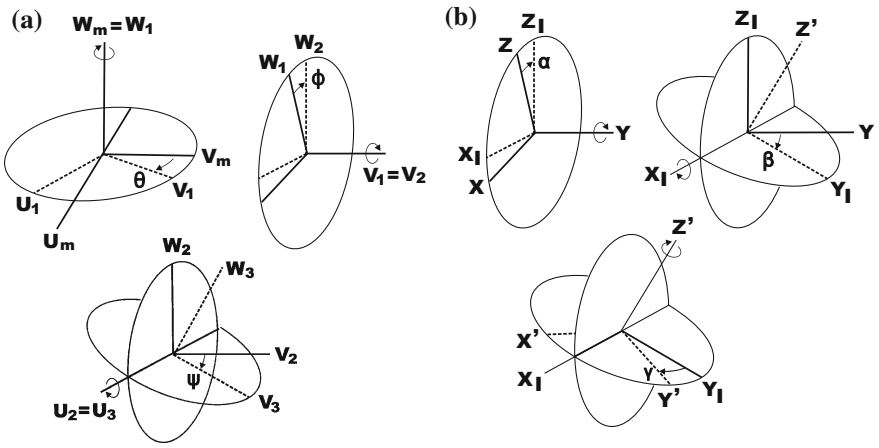

Fig. 4.7 Definition of the coordinate rotations: **a** double rotation (both upper figures) including a possible third rotation (*below*), the measurement parameters are described with m and the numbers indicate the rotations; **b** planar-fit method according to Wilczak et al. (2001), consisting in two rotations after a linear multiple regression (both upper figures) followed by a rotation into the mean wind field (*below*), with the index I describing subrotations and the apostrophe the coordinates after rotation (Adapted from Wilczak et al. 2001, with kind permission of © Kluwer Academic Publisher B. V. Dordrecht 2001, All rights reserved)

With these rotations, the coordinate system of the sonic anemometer is aligned with the streamlines. Over flat terrain, these rotations correct errors in the vertical orientation of a sonic anemometer. In sloped terrain, the streamlines are not implicitly normal to the gravity force, and at least for short averaging periods rotations may be questionable. This is especially true for short convective events or for flow distortion problems of the sensor, which may significantly affect the vertical wind components, but are not associated with the coordinate rotations. For convection or periods of low wind velocities, rotation angels up to 20–40° are typical.

Therefore, the two-rotation approach requires certain quality control procedures. However, it is the standard method in many routine monitoring networks due to its easy application (Rebmann et al. 2012). If the data are screened for low wind velocities (see Sect. 4.2.6) questionable large rotation angles are also excluded.

The third rotation (Fig. 4.7a, below) around the new x-axis was proposed by McMillen (1988) to eliminate the covariance from the vertical and the horizontal, normal to the mean wind direction, wind component (Kaimal and Finnigan 1994)

$$\begin{aligned} u_3 &= u_2, \\ v_3 &= v_2 \cos\psi + w_2 \sin\psi, \\ w_3 &= -v_2 \sin\psi + w_2 \cos\psi, \end{aligned} \tag{4.43}$$

where

$$\psi = \tan^{-1}\left(\frac{\overline{v_2 w_2}}{\overline{v_2^2} - \overline{w_2^2}}\right). \tag{4.44}$$

This rotation does not significantly influence the fluxes, and introduces some problems. Therefore, it is recommended to use only the first two rotations (Aubinet et al. 2000).

A rotation into the mean stream lines was proposed by Paw U et al. (2000) and Wilczak et al. (2001). With this so called planar-fit method, the differences between the anemometer alignment and the mean stream field for a given measurement site is estimated over a long time period (days to weeks). The mounting and orientation of the anemometer should not change over this period. It is therefore recommended to combine the sonic anemometer with an inclinometer and to observe the inclinometer data regularly. If necessary, the anemometer must be regularly realigned with its initial orientation.

A matrix form is suitable to describe the planar-fit method (Wilczak et al. 2001)

$$\vec{u}_p = P(\vec{u}_m - \vec{c}), \tag{4.45}$$

where $\vec{u}_m$ is the vector of the measured wind velocities, $\vec{u}_p$ is the vector of the planar-fit rotated wind velocities, $\vec{c}$ is an offset vector, and P is a transformation matrix. The equations of rotations are then:

$$\begin{aligned}
\overline{u_p} &= p_{11}(\overline{u_m} - c_1) + p_{12}(\overline{v_m} - c_2) + p_{13}(\overline{u_m} - c_3) \\
\overline{v_p} &= p_{21}(\overline{u_m} - c_1) + p_{22}(\overline{v_m} - c_2) + p_{23}(\overline{w_m} - c_3) \\
\overline{w_p} &= p_{31}(\overline{u_m} - c_1) + p_{32}(\overline{v_m} - c_2) + p_{33}(\overline{w_m} - c_3)
\end{aligned} \tag{4.46}$$

The offset vector is necessary because, for example, the flow distortion of the sonic anemometer generates a slightly positive vertical wind velocity (Dyer 1981), and therefore a value of c_3 which differs from zero. The offset of the horizontal wind components can be assumed negligible. Nevertheless, before using a sonic anemometer the offset values during calm conditions (or observed in a box) should be controlled and if necessary corrected (see Sect. 6.2.2).

The planar-fit coordinate system fitted to the mean-flow streamlines is characterized by $\overline{w_p} = 0$. The tilt angels can be calculated according Eq. (4.46) with multiple linear regressions

$$\overline{w_m} = c_3 - \frac{p_{31}}{p_{33}}\overline{u_m} - \frac{p_{32}}{p_{33}}\overline{v_m}, \tag{4.47}$$

where $p_{31} = \sin\alpha$, $p_{32} = -\cos\alpha \sin\beta$ and $p_{33} = \cos\alpha \cos\beta$. Knowing these angles, the coordinate system can be rotated according to Fig. 4.7b, above, in the proposed order. This means that the rotation is first around angle α and then around β. The rotation

angles for this method are only a few degrees. If the rotation angels differ for different wind directions and velocities, then this method must be applied for single wind sectors and velocity classes. Of special importance is the length of the period for which the coordinate rotation should be applied. Dependent on the canopy structure (deciduous forest) and other factors this length must be individually determined (Su et al. 2008; Siebicke et al. 2012). Therefore, with the planar-fit method fluxes cannot be measured in real time.

After the rotation into the mean streamline level, each single measurement must be rotated into the mean wind direction according to (Fig. 4.7b, below):

$$\gamma = \arctan\left(\frac{\overline{v_p}}{\overline{u_p}}\right) \tag{4.48}$$

This is an absolute analogue to other rotation methods, but is applied as last step. In general, for the single measurements a block averaging over 30 min is used.

4.2.3.3 Spectral Correction in the High Frequency Range

An important correction to the actual available turbulence spectra is the adjustment of the spectral resolution of the measurement system. Hence, the time resolution (time constant) of the sensor, the measurement path length, and the separation between different measurement paths must be corrected. Currently, the correction method according to Moore (1986) is usually applied (Foken et al. 2012c), but it should be noted that the published software program has errors. Thus, the stability-dependent spectral function must be taken from the original source (Kaimal et al. 1972), see Sect. 2.5. Furthermore, the published aliasing correction should not be applied. The spectral functions are based on a few measurements from the Kansas experiment, and therefore its universal validity is limited.

The spectral correction is made using transfer functions (see Sect. 6.1.3). For each combination of the path length for the vertical wind velocity of a sonic anemometer (w) and the sensor for the determination of the relevant flux parameter (x), there are separate filters for the time constant (τ), the measurement path length (d), and the senor separation (s), which must be determined. The product of these single functions is the total transfer function:

$$T_{w,x}(f) = \sqrt{T_{\tau,w}(f)}\,\sqrt{T_{\tau,x}(f)}\,\sqrt{T_{d,w}(f)}\,\sqrt{T_{d,x}(f)}\,T_{s,w,x}(f) \tag{4.49}$$

If the sensors are aligned parallel to the mean wind, the spectral correction is partially done using the above-mentioned cross-correlation correction.

The method can also be applied using different transfer functions according to Horst (1997) and Moncrieff et al. (1997). A comparison of both methods was presented by Fratini and Mauder (2014). For a chosen measurement system, it is also possible to use a simple analytical correction for a site that takes into account

the observed spectra (Massman 2000). From Eugster and Senn (1995), a method was proposed which is based on an electronic damping circuit.

4.2.3.4 Spectral Correction in the Low Frequency Range

Often a sampling time of 30 min is not long enough to measure the low frequency part of the fluxes. In principle, the averaging interval can be extended by an elimination of a trend, and in most cases it is sufficient to subtract only the linear trend. This of course involves the danger that the low frequency events, which are not associated with turbulent fluxes, contribute to the calculated flux (Finnigan et al. 2003).

It is therefore advised to test if the flux has its maximum value within the usual averaging time. This is done using the so called *ogive* test (Desjardins et al. 1989; Oncley et al. 1990; Foken et al. 1995). It is calculated using the cumulative integral of the co-spectrum of the turbulent flux beginning with the highest frequencies:

$$Og_{w,x}(f_0) = \int_{\infty}^{f_0} Co_{w,x}(f)df \tag{4.50}$$

If the value of the integral approaches a constant value (flux) for low frequencies, and if an enhancement of the averaging interval gives no significant changes, then no additional correction is necessary (Fig. 4.8).

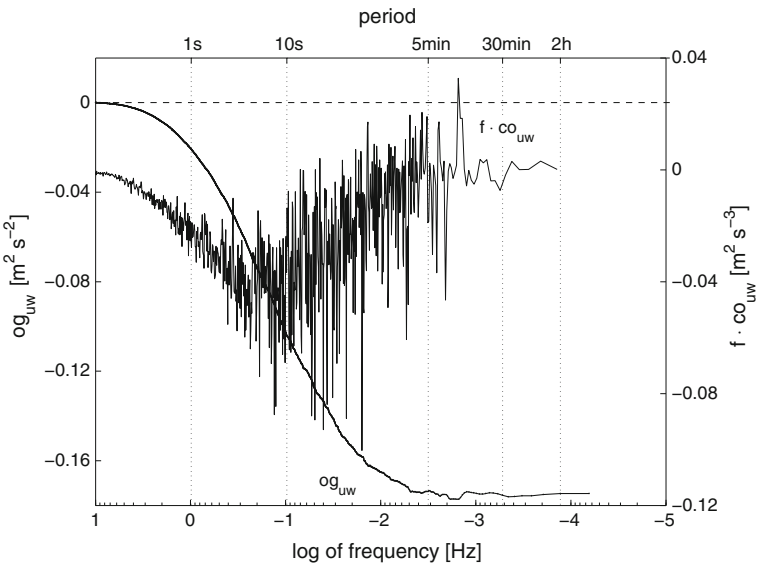

Fig. 4.8 Converging ogive (Og_{uw}) and co-spectrum ($f\,CO_{uw}$) of the momentum flux during the LITFASS-2003 experiment (June 09, 2003, 12:30–16:30 UTC, Foken et al. 2006, published with kind permission of © Authors 2006, CC Attribution 3.0 License, All rights reserved)

For the LITFASS-2003 experiment, the ogive converged within an averaging time of 30 min in about 80% of all cases (Foken et al. 2006; Charuchittipan et al. 2014). In the remaining cases, which occurred mainly during the transition periods of the day when fluxes are typically low, the ogives did not converge or reached a maximum value before the integration time of 30 min, and then decreased. By applying the ogive correction for low frequency fluxes of the investigated data set, the fluxes would increase less than 5%. The ogive correction is currently not routinely applied.

4.2.3.5 Correction of the Buoyancy Flux

The temperature measured with sonic anemometers is the so-called sonic temperature (Kaimal and Gaynor 1991):

$$T_s = T(1 + 0.32\, e/p) \tag{4.51}$$

It differs only slightly from the virtual temperature (see Eq. 2.14):

$$T_v = T(1 + 0.38\, e/p) \tag{4.52}$$

Therefore, the heat flux measured with the sonic temperature is approximately equal to the buoyancy flux. To transfer the measured buoyancy flux into the sensible heat flux, the Reynolds decomposition of Eq. (4.51) must be used in Eq. (4.33). It must be noted that the sound signal is modified depending on the construction of the sonic anemometer and the cross wind velocity. Schotanus et al. (1983) developed a correction method which is widely used. Analogue to the WPL correction, which is described in the following section, it should be named SND-correction after the three developers *S*chotanus, *N*ieuwstadt, and *D*eBruin. It is valid only for vertical measurement paths. For currently available sonic anemometers, Liu et al. (2001) adapted the method including the so called crosswind correction:

$$\rho c_p \left(\overline{w'T'}\right) = \rho\, c_p \frac{\overline{w'T'_s} + \frac{2\overline{T}}{c^2}\left(\overline{u}\,\overline{u'w'}\,A + \overline{v}\,\overline{v'w'}B\right)}{1 + \frac{0.51\,\overline{T}c_p}{\lambda\, Bo}} \tag{4.53}$$

Because most of the producers include the crosswind correction in the sensor software, the second term in the enumerator of Eq. (4.53) can be neglected. The coefficients A and B for different types of sonic anemometers are given in Table 4.11.

Table 4.11 Coefficients for Eq. (4.53) according to Liu et al. (2001), φ: angle between the measurement axis and the *horizontal line* for different presently used sonic anemometer types. Except for the USA-1 without turbulence module, these corrections are already included in the sensor software

Factor	CSAT3	USA-1	Solent	Solent-R2
A	7/8	3/4	$1–1/2 \cdot \cos^2\varphi$	½
B	7/8	3/4	$1–1/2 \cdot \cos^2\varphi$	1

4.2.3.6 WPL-Correction

Webb et al. (1980), discussed the necessity for a density correction (*WPL*-correction according to *W*ebb, *P*earman, and *L*euning, formerly also called Webb-correction), which is caused by ignoring density fluctuations, a finite humidity flux at the surface, and the measurement of gas concentration per volume unit instead of per mass unit. A review of the continuing discussions over the last 20 years is given by Fuehrer and Friehe (2002). A different approach uses density-weighted averaging according to Hesselberg (1926), Kramm et al. (1995), and Kramm and Meixner (2000). However, the application of this approach would lead to inconsistencies in this book; therefore in the following, the version by Webb et al. (1980) is used. Webb et al. (1980) begin their derivation assuming dry air while Bernhardt and Piazena (1988) assume moist air. The differences between both methods are negligible. Nevertheless, recently several critical notes related to the *WPL* correction were published (see Sect. 4.2.4). Therefore Leuning (2007) summarized the method again (see also Foken et al. 2012c).

The total flux measured per unit mass, must be represented by the specific content of the matter q_c, according to the relation

$$F_c = \overline{\rho w q_c} = \overline{\rho w}\,\overline{q_c} + \overline{(\rho w)' q_c'}. \tag{4.54}$$

Using the partial density

$$\rho_c = \rho\, q_c \tag{4.55}$$

the relation per unit volume is

$$F_c = \overline{\rho w q_c} = \overline{w}\,\overline{q_c} + \overline{w' \rho_c'}, \tag{4.56}$$

which is applied in measurements. The mean vertical wind velocity is included in a correction term, which is given in the following form (Webb et al. 1980; Foken et al. 2012c):

$$F_c = \overline{w' \rho_c'} + 1.61\,\frac{\overline{\rho_c}}{\overline{\rho_w}}\overline{w' \rho_w'} + (1 + 1.61\overline{q})\,\frac{\overline{\rho_c}}{\overline{T}}\overline{w' T'}, \tag{4.57}$$

with $M_L/M_w = 1.61$. Thus, it this follows that the measurement of trace gas fluxes always requires simultaneous measurements of the water vapour concentration and the latent heat flux. For the measurement of the latent heat flux a simpler equation can be applied:

$$\frac{Q_E}{\lambda \rho} = (1 + 1.61\,\overline{q})\left(\overline{w'\rho w'} + \frac{\overline{\rho_c}}{\overline{T}}\overline{w'T'}\right), \tag{4.58}$$

The WPL-correction is large if the turbulent fluctuations are small relative to the mean concentration. For example, this is the case for carbon dioxide where corrections up to 50% are typical. For water vapour flux, the corrections are only a few percent because the effects of the Bowen ratio and the sensible heat flux balance each other (Liebethal and Foken 2003, 2004).

The conversion from volume into mass-related values using the WPL-correction is not necessary if the water vapour concentrations or the concentrations of other gases are transferred into mol per mol dry air before the eddy-covariance is calculated. Some manufacturers offer this sensor-internal conversion. The WPL-correction can be omitted for closed path sensors and if heated tubes that eliminate temperature fluctuations are used. However, this must be controlled and possibly corrected (Leuning and Judd 1996; Ibrom et al. 2007a; Foken et al. 2012c), otherwise too low fluxes are measured.

4.2.4 Corrections in Question

4.2.4.1 Flow Distortion Correction

Already Dyer (1981) pointed out that sonic anemometers generate a small updraft, which can be corrected with a coordinate rotation (see Sect. 4.2.3.2). The applications of the flow distortion correction need some care because these are determined in the wind tunnel, but these corrections have much lower values in the atmosphere (Högström and Smedman 2004). In the literature the transducer correction and the angle of attack correction are discussed.

4.2.4.2 Transducer Correction

Disturbances of the wind field are the most important sources of errors for sonic anemometers. The reasons are the installations of the sensors and the size of the transducers. For new sensors, a large ratio of the path length, d, to the transducer diameter, a, of up to $d/a = 50$ is required, because under these circumstances the influences of flow distortion are small. Furthermore, the angle, θ, between the wind vector and the path should be large. The results are based on wind tunnel

investigations of Kaimal (1978) and Kaimal et al. (1990) for a sonic anemometer with orthogonal measurement paths. For a ratio $d/a = 15$, the deviations are (Kaimal and Finnigan 1994):

$$(u_d)_{means} \begin{cases} u_d(0.82 + 0.18 \cdot \theta/75), & 0^\circ \leq \theta \leq 75^\circ \\ u_d, & 75^\circ \leq \theta \leq 90^\circ \end{cases} \tag{4.59}$$

Due to these results the vertical wind velocity should not be measured with a vertical path but with a path that is not affected by the wind direction (omni-directional, Fig. 6.14, Zhang et al. 1986).

Recently some papers explained a reduction of the vertical wind velocity by a transducer effect (Frank et al. 2013; Horst et al. 2015) and proposed to apply corrections similar to Eq. (4.59). These measurements were not done in a wind tunnel and a benchmark is missing. Therefore, applying these corrections is not recommended.

4.2.4.3 Angle of Attack Correction

The angle of attack correction assumes that turbulence elements move through the sonic anemometer on waveform patterns and thus reach the anemometer at a specific angle. As a consequence, the vertical and horizontal wind component should be highly correlated, which is however not the case (see Sect. 4.2.5). Nakai et al. (2006) developed a correction approach in the wind tunnel. The measurements were repeated in a turbulent field with inclined sonic anemometers (Nakai and Shimoyama 2012), but the measurement setup was questionable. The correction should only be applied with care. Only corrections for non-inclined streamlines that correct the effects of anemometer mounts should be used.

4.2.4.4 Modification of the WPL-Correction

Using an alternative approach based on moist air, Liu (2005) found significant differences in the corrections of carbon dioxide fluxes. However, Kowalski (2006), Massman and Tuovinen (2006), and Leuning (2007) have shown that this alternative correction is based on wrong assumptions.

Liu also proposed a correction of the energy balance closure (see Sect. 3.8, Liu et al. 2006), which is however based on the correction with the Bowen-ratio method (Twine et al. 2000). Assuming more realistic corrections for energy balance closure, this method would be definitely applicable.

4.2.4.5 Correction of the Specific Heat

Due to the presentation by Stull (1988) of the correction of humidity-dependent fluctuations of the specific heat proposed by Brook (1978), which is some percentage of the flux, this correction is often used. However, shortly after the publication of this correction several authors (Leuning and Legg 1982; Nicholls and Smith 1982; Webb 1982) showed the this correction is based on incorrect conditions, and should never be used.

4.2.4.6 Advection Correction

Matter exchange and especially vertical fluxes in complex terrain motivated the advection corrections proposed by Lee (1998). This correction increases the low fluxes at night by application of the following equation for the vertical advection

$$F_{VA} = \overline{w}\left[\overline{\chi_c(Z_m)} - \overline{\chi_c}\right] \tag{4.60}$$

where $\overline{\chi_c}$ is the mixing ratio measured from the ground up to the measurement height. The discussion has shown (Finnigan 1999; Paw U et al. 2000) that the vertical advection cannot be separated from other advection terms as shown in Sect. 3.6. The correction is no longer recommended (Foken et al. 2012c).

4.2.4.7 Burba Correction

Erroneous measurements with open-path gas analysers for low temperatures triggered investigations of the effects of free convection on the measured flux between the heated radiation source and the receiver (LiCor 7500, Grelle and Burba 2007) and to formulate a correction (Burba et al. 2008). At times, these corrections were found to be too large (Järvi et al. 2009; Oechel et al. 2014). Additionally, miss-interpretations may have affected the derivation. Thus, applying the correction is not recommended. Instead, open-path gas analysers should be tilted such that any possible convection does not reach the receiver. Furthermore, the temperature of the radiation source was reduced by the producer.

4.2.5 Quality Assurance

Turbulence measurements with the eddy-covariance method cannot be controlled in a simple way with plausibility tests (see Sect. 6.3.1). The quality assurance of turbulence measurements is a combination of the complete application of all corrections and the exclusion of meteorological influences such as internal boundary

layers, gravity waves, and intermitted turbulence. The main aim of the control of the data quality is to validate if, under given meteorological conditions, the simplifications of Eq. (4.32) are warranted (see Sect. 2.1.2). Quality tests (Kaimal and Finnigan 1994; Foken and Wichura 1996; Foken et al. 2004) are used to validate the theoretical assumptions of the method such as steady-state conditions, homogeneous surfaces, and developed turbulence.

For the eddy-covariance method, steady states are required. Meteorological measurements fulfil these conditions for short time periods up to one hour only roughly. There are several tests, which can be used directly or indirectly. For example, stationarity can be determined by examining the fluxes for different averaging times (Gurjanov et al. 1984; Foken and Wichura 1996). In this way, the flux is determined once over M short intervals each of only about 5 min duration, and then the average over the short time intervals is calculated (Remark: $\left[\overline{x'y'}\right]_{5min}$ means that this is a 30 min average calculated from 5 min averages):

$$\begin{aligned} \left(\overline{x'y'}\right)_i &= \frac{1}{N-1}\left[\sum_j x_j y_j - \frac{1}{N}\left(\sum_j x_j \sum_j y_j\right)\right] \\ \left[\overline{x'y'}\right]_{5\,\mathrm{min}} &= \frac{1}{M}\sum_j \left(\overline{x'y'}\right)_i \end{aligned} \tag{4.61}$$

Next, the flux is calculated over the whole averaging interval (e.g. 30 min):

$$\left[\overline{x'y'}\right]_{30\,\mathrm{min}} = \frac{1}{M\cdot N-1}\left\{\sum_i\left(\sum_j x_j\cdot y_j\right)_i - \frac{1}{M\cdot N}\left[\sum_i\left(\sum_j x_j\right)_i \cdot \sum_i\left(\sum_j y_j\right)_i\right]\right\} \tag{4.62}$$

Steady-state conditions can be assumed, if both results do not differ by more than 30%. A gradation of the differences can be used as a classification of the data quality:

$$Stat = \left|\frac{\left[\overline{x'y'}\right]_{5\,\mathrm{min}} - \left[\overline{x'y'}\right]_{30\,\mathrm{min}}}{\left[\overline{x'y'}\right]_{30\,\mathrm{min}}}\right| \cdot 100\% \tag{4.63}$$

From Vickers and Mahrt (1997), two tests were proposed, which give similar results. They calculate the skewness and excess of the time series. For values of skewness $>|2|$ and values of excess <1 and >8, the authors suggested a bad data quality, and for skewness $>|1|$ and excess <2 and >5 medium data quality is assumed. For wind components, the data at the beginning and end of a time series are compared. The difference of these values normalized by the mean wind velocity must fulfill the relation

$$\left|\frac{u_1 - u_N}{\bar{u}}\right| < 0.5, \tag{4.64}$$

if the time series can be accepted as steady-state. This method does not always correctly identify unsteady conditions in the middle of the measurement interval.

The steady-state test often identifies large sudden jumps in the signal, a constant signal for a certain time, or changes of the signal level. The reason for these events is often an electronic one. Mahrt (1991) proposed a test using the Haar-wavelet for which the time of events can be well located. The test can also identify periods of intermittent turbulence.

The development of the turbulence can be investigated with the flux-variance similarity described in Sect. 2.4 (Foken and Wichura 1996). In this case, the measured integral turbulence characteristics (ITC) are compared with the modelled characteristics according to Tables 2.13 and 2.14. A good data quality is assumed for differences less than about 30%.

$$ITC = \left| \frac{\left(\frac{\sigma x}{X_*}\right)_{Modell} - \left(\frac{\sigma x}{X_*}\right)_{Messung}}{\left(\frac{\sigma x}{X_*}\right)_{Modell}} \right| \cdot 100\% \tag{4.65}$$

In a similar way, the comparison of the correlation coefficient between values used in the flux calculations with the mean values can be used for quality assurance testing (see Table 4.16 in Sect. 4.3, Kaimal and Finnigan 1994).

Additionally, the wind components should be included in a system of quality control tests. The mean vertical wind must be low such that over flat terrain and for horizontal wind velocities <5 m s^{-1} it is <0.15–0.20 m s^{-1}. For sonic anemometers with a limited range of acceptable wind directions, measurements within an inflow sector that is affected by instrument mounts should be excluded. The excluded region should be based on the typical standard deviation of the wind direction at a particular site and given micrometeorological conditions, but is typically ±30–40°. For sonic anemometers with unlimited inflow angles (omni-directional) the flow through instrument mounts and sensor heads can reduce the overall data quality.

An evaluation system for turbulent fluxes consists of two steps: The single tests should be evaluated according to the threshold values and corresponding data quality classes (Table 4.12) and the overall quality of a measurement is expressed as an appropriate combination of the single tests (Table 4.13). The highest priority should be given to the steady-state test. Note that for the test on integral turbulence characteristics for neutral stratification, the errors in the determination of the characteristics for scalars can be very high. This test should not be overly interpreted, and the test on the characteristics of the wind parameters should dominate. In any case, the classification results of the single tests should be stored to have them available later in cases of doubt. The classification according to Table 4.12 was done such that classes 1–3 have a high accuracy and the data can be used for basic research. Classes 1–6 can be used for long-term measurements of fluxes

Table 4.12 Classification of the data quality of the steady-state test according to Eq. (4.63); the comparison of the integral turbulence characteristics with model assumptions according to Eq. (4.65) and Tables 2.13 and 2.14, and the wind criteria, for example for the sonic anemometer CSAT3 (Foken et al. 2004, 2012c)

Steady state, differences		Integral turbulence characteristics, differences		Horizontal inflow sector for CSAT3	
Class	Range (%)	Class	Range (%)	Class	Range (°)
1	0–15	1	0–15	1	±0–30
2	16–30	2	16–30	2	±31–60
3	31–50	3	31–50	3	±60–100
4	51–75	4	51–75	4	±101–150
5	76–100	5	76–100	5	±101–150
6	101–250	6	101–250	6	±151–170
7	251–500	7	251–500	7	±151–170
8	501–1000	8	501–1000	8	±151–170
9	>1000	9	>1000	9	>±171

Table 4.13 Proposal for the combination of single quality tests (Table 4.12) to an overall data quality of flux measurements (Foken et al. 2004, 2012c)

Overall quality	Steady state	Integral turbulence characteristics	Horizontal inflow sector
1	1	1–2	1–5
2	2	1–2	1–5
3	1–2	3–4	1–5
4	3–4	1–2	1–5
5	1–4	3–5	1–5
6	5	≤ 5	1–5
7	≤ 6	≤ 6	≤ 8
8	≤ 8 ≤ 8	≤ 8 6–8	≤ 8 ≤ 8
9	One ranging 9		

without limitations. Measurements of the classes 7–8 should only be used for ballpark estimates and should, if necessary, be deleted while data in class 9 are always removed. In several papers, certain classes were also combined (Rebmann et al. 2005; Mauder et al. 2013).

With the discussed approach, any erroneous measurements should be successfully detected and removed. If this is not the case, or if the tests can only be partially applied, it is possible to screen the data using final tests (Papale et al. 2006).

Analogue to Eq. (4.38), this final screening also uses the absolute deviation from the median *MAD* but the parameter q can be reduced (4 or 5.5).

4.2.5.1 Gap Filling

The application of the eddy-covariance method in long-term measurement programs such as the international FLUXNET programme (Baldocchi et al. 2001) requires objective methods on how to handle missing data. This is because with such measurement programs annual sums such as the Net Ecosystem Exchange (NEE) are determined. In substance, two types of missing data must be corrected. One type is missing data from single systems due to meteorological influences such as heavy rain or failure of the whole system. The second type is data that must be replaced. If, for example, during the night no turbulent exchange conditions exist, then the measurement method no longer works satisfactorily. For the measurements of carbon dioxide fluxes, the methods of gap filling are well developed (Falge et al. 2001; Hui et al. 2004; Gu et al. 2005; Reichstein et al. 2005; Moffat et al. 2007; Lasslop et al. 2010). Nevertheless these methods, which use an approach for the carbon assimilation at daytime and a different approach for respiration, are still under discussion. Recently, gap filling with models (e.g. Papale and Valentini 2003) are applied.

The determination of the carbon uptake (NEE) at daytime takes place with the so called Michaelis-Menton function (Michaelis and Menton 1913; Falge et al. 2001), which must be evaluated for different temperature classes and the global radiation:

$$Q_{c,Tag} = \frac{a\,K\downarrow\, Q_{c,sat}}{a\,K\downarrow\, + Q_{c,sat}} + Q_{R,Tag} \tag{4.67}$$

where $Q_{c,sat}$ is the carbon flux for light saturation ($K\downarrow = \infty$), Q_R is the respiration at daytime, and a and $Q_{c,sat}$ must be determined with multiple regression using data from an available dataset for the specific measurement site.

The respiration of an ecosystem can be determined with the Lloyd-Taylor-function (Lloyd and Taylor 1994; Falge et al. 2001)

$$Q_R = Q_{R,10} e^{E_0\left[\frac{1}{283.15K - T_0} - \frac{1}{T - T_0}\right]}, \tag{4.68}$$

where $Q_{R,10}$ is the respiration at 10 °C, T_0 = 227.13 K (Lloyd and Taylor 1994), and E_0 describes the temperature dependence of the respiration. The parameters of this equation are determined from nighttime ($K\downarrow$ < 10 W m^{-2}) eddy-covariance measurements with the assumption that for such low radiation fluxes only the respiration can be measured. The coefficients are determined also for temperature classes (Fig. 4.9).

While the Michaelis-Menton function is in general used for gap filling for the daytime, the Lloyd-Taylor function must be used at night because of low

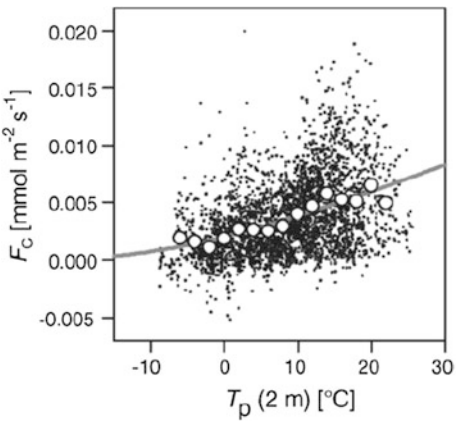

Fig. 4.9 Calculation of the respiration from NEE measurements at night as a function of air temperature at 2 m height according to Eq. (4.67), *grey line*. Circles are the medians of 2°-classes, points are individual values (Adapted from Ruppert et al. 2006b, with kind permission of © Elsevier Science AG Oxford 2006, All rights reserved)

turbulence. The decision regarding the application follows from the so called u_*-criterion (Goulden et al. 1996). Therefore, the respiration is normalized to exclude the temperature sensitivity using a model calculation according to Eq. (4.67), and plotted as a function of the friction velocity u_*. Above a certain friction velocity, the normalized respiration is constant. Measurements with a lower friction velocity are gap filled. Typical threshold values are in the range $u_* = 0.3–0.4$ m s^{-1}. However, such a threshold value cannot be determined for all stations (Gu et al. 2005).

It must be noted that for both methods the equations for the carbon flux during the day and the respiration during the night are climatological parameterizations. These can have significant differences from the individual values. The determination of the respiration relationships is particularly difficult because of the large scatter of the data (Fig. 4.9). It is recommended to use medians for the temperature classes. Due to the application of the u_*-criterion only few data are available with low turbulent conditions. Therefore, an over-parameterization of the respiration may be possible. Very critical is the situation in winter, when many data are missing. In this case, data for many years should be used for the calculation of the parameterization. Also the assimilation is difficult to parametrize in winter time, because the parametrization is based on few sunny weather periods. It is very useful to set the assimilation to zero for periods without biological activity if the investigations aim at the determination of annual sums (Lindauer et al. 2014).

A more objective approach seems to be the application of the quality criterion for turbulent fluxes as introduced in Sect. 4.1.3 (Ruppert et al. 2006b). According to this, very high data quality is used to determine the Michaelis-Menton and Lloyd-Taylor functions. Then both functions are used to fill gaps of data with low data quality. The benefit of this method is that nighttime data with high data quality and low friction velocity can be used to parameterize the Lloyd-Taylor function. On the other hand, daytime values with low data quality must be gap filled. However, this approach requires the availability of raw data.

For the gap filling of evapotranspiration data the modelling with the Penman-Monteith-approach or, if using a correction factor, also with the Priestley-Taylor-approach can be applied (see Sect. 5.1.2).

4.2.6 Overall Evaluation

Due to the very complicated algorithms of the eddy-covariance method, errors cannot easily be estimated according to the error propagation law (Huges and Hase 2010). Nevertheless Mauder et al. (2006) have tried using sensor and software comparisons during the experiments EBEX-2000 and LITFASS-2003 to determine the accuracy of the measurement method. A significant dependence was found on the type of sonic anemometer (compare Table 6.8) and on the data quality. The results are summarized in Table 4.14.

Hollinger and Richardson (2005) have tried to evaluate the uncertainty of the eddy-covariance method using data from two instrumented towers with the same footprint. For climatological analyses, a comparison of different years is possible (Richardson et al. 2006). Quite promising are statistical methods. Hereby, it must be noticed that the time series used for the eddy-covariance are auto-correlated and the usual statistical criterions for random numbers cannot be applied (Bartels 1935). Approaches by Lenschow et al. (1994) and Finkelstein and Sims (2001) obviously account for this limitation. Thus, according to Mauder et al. (2013) the noise of the errors εx and εy is

$$\sigma_{covariance}^{noice} = \sqrt{\frac{1}{N}}\sqrt{\overline{\varepsilon x^2 y'^2} + \overline{\varepsilon y^2 x'^2}} \tag{4.68}$$

and the statistical error following the error propagation law (Huges and Hase 2010), e.g. for the friction velocity, is

$$\sigma_\tau = \frac{\rho}{u_*}\sqrt{\overline{u'w'}^2 \sigma^2_{\overline{u'w'}} + \overline{v'w'}^2 \sigma^2_{\overline{v'w'}}}. \tag{4.69}$$

Table 4.14 Evaluation of the accuracy of the eddy-covariance method on the basis of the results of the experiments EBEX-2000 and LITFASS-2003 (Mauder et al. 2006) dependent on the data quality (Sect. 4.2.5) and from the type of the sonic anemometer (Table 6.8, Foken and Oncley 1995)

Sonic anemometer	Data quality class	Sensible heat flux	Latent heat flux
Type A, e.g. CSAT3	1–3	5% or 10 W m^{-2}	10% or 20 W m^{-2}
	4–6	10% or 20 W m^{-2}	15% or 30 W m^{-2}
Type B, e.g. USA-1	1–3	10% or 20 W m^{-2}	15% or 30 W m^{-2}
	4–6	15% or 30 W m^{-2}	20% or 40 W m^{-2}

Table 4.15 Evaluation of the eddy-covariance method

Criterion	Evaluation
Area of application	Basic research and expensive continuous measurement programs
Financial expense	10–50 k€ per system
Personal expense	Continuous scientific and technical support
Education	Good micrometeorological and measurement technique knowledge
Error	Depending on the micrometeorological conditions 5–10%
Sampling	10–20 Hz
Time resolution of fluxes	10–60 min
Application for chemical compounds	Selected inert gases (gas analysers with high time resolution)
Restrictions in the application	Sufficient footprint area, turbulent conditions necessary, depending on the senor, possible precipitation

The method leads to results comparable with Table 4.14. Systematic errors essentially are the unclosed energy balance (see Sect. 3.8) and a limited footprint (see Sect. 3.4).

It is seen that the eddy-covariance method (Table 4.15) is the only direct measurement method and the most accurate with the largest time resolution. However, it needs also the most comprehensive knowledge and great experimental effort.

4.3 Flux-Variance Relations

The flux-variance relation (variance method) according to Sect. 2.4 allows the calculation of fluxes using the measured variance of a meteorological parameter and the integral turbulence characteristics. Many investigations of this method have been made. However, the variance method has never reached a practical relevance even though the method has an accuracy comparable to the eddy-covariance method (Tsvang et al. 1985). Thus, the application of the variance method according to Eqs. (2.105) and (2.106) as well as Tables 2.13 and 2.14 is possible.

The equations can also be derived from the definition of the correlation coefficient or the covariance. Therefore, the method is often called eddy-correlation method, which should not be confused with the eddy-covariance method:

$$r_{wX} = \frac{\overline{w'X'}}{\sigma_w \, \sigma_X} = \frac{F_X}{\sigma_w \, \sigma_X} \tag{4.70}$$

$$r_{wY} = \frac{\overline{w'Y'}}{\sigma_w \, \sigma_Y} = \frac{F_Y}{\sigma_w \, \sigma_Y} \tag{4.71}$$

Table 4.16 Typical values of the correlation coefficient between the vertical and horizontal wind components and between vertical wind component and temperature

Author	r_{uw}	r_{wT}
Kaimal and Finnigan (1994)	−0.35	0.5 (unstable) −0.4 (stable)
Arya (2001)	−0.15	0.6 (unstable)

By assuming the same values for the correlation coefficients (Table 4.16), well-known standard deviations, and one well-known flux, a second flux can be determined. The sign of the flux must be determined by additional measurements, e.g. by measurements of the temperature gradient:

$$|F_X| = |F_Y| \frac{\sigma_X}{\sigma_Y} \tag{4.72}$$

The standard deviations can be determined using a lower frequency spectral range, than the necessary spectral range of the eddy-covariance method for the reference flux. This method can, for example, be applied, if only one of the two gas fluxes can be measured with high time resolution using the eddy-covariance method.

Furthermore the flux can also be determined according to Eq. (4.65), if the correlation coefficient is well known:

$$F_X = r_{wX} \sigma_w \, \sigma_X \tag{4.73}$$

The correlation coefficient can be roughly parameterized according to the stratification (Table 4.16)

$$r_{wX} = \tilde{\varphi}(\varsigma). \tag{4.74}$$

But the parameterization lacks a sufficient data basis.

An evaluation of the practically rarely used flux-variance method is given in Table 4.17. Due to the methodical and technical progress of the eddy-covariance method, this method has only historical relevance.

4.4 Accumulation Methods

4.4.1 Eddy-Accumulations-Method (EA)

The basic idea of the eddy-accumulation method (conditional sampling) originates in the work of Desjardins beginning in 1972 (Desjardins 1977). He assumed that the covariance of the turbulent flux could be averaged separately for positive and negative vertical wind velocities:

Table 4.17 Evaluation of the flux-variance method

Criterion	Evaluation
Area of application	Basic research
Financial expense	2–10 k€ per system
Personal expense	Continuous scientific and technical support
Education	Good micrometeorological and measurement technique knowledge
Error	Depending on the micrometeorological conditions 10–30%
Sampling	10–20 Hz (probably lower)
Time resolution of fluxes	10–30 min
Application for chemical compounds	Selected inert gases (gas analysers with high time resolution)
Restrictions in the application	Sufficient footprint area, turbulent conditions necessary, if necessary similarity of the scalars

$$\begin{aligned} \overline{w'c'} &= \overline{w^+c} + \overline{w^-c} = (\overline{w^+} + \overline{w^-})\bar{c} + \overline{w^+c'} + \overline{w^-c'} \\ (\overline{w^+} + \overline{w^-}) &= \bar{w} = 0 \end{aligned} \tag{4.75}$$

Realization of this direct measurement technique should be done by concentration measurements in two separate reservoirs for positive and negative vertical wind velocities weighted with the actual vertical wind velocity (Fig. 4.10). However, the therefore necessary valve control technology did not yet exist.

However, the conditional sampling method has still a practical relevance in data analysis. For data with a high temporal resolution of the vertical wind velocity and a scalar, the time series can be conditionally sampled according to Eq. (4.75). If it is possible to fulfil the condition $\overline{w} = 0$, fluxes can be calculated without the assumption of steady state conditions.

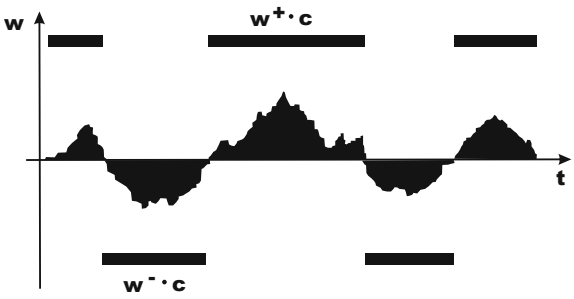

Fig. 4.10 Schematic view of the eddy-accumulation method (Adapted from Foken et al. 1995, with kind permission of © Gebr. Borntraeger Verlagsgesellschaft Stuttgart 1995, www.schweizerbart.de, All rights reserved)

4.4.2 Relaxed Eddy-Accumulation Method (REA)

The work of Businger and Oncley (1990) was a technical breakthrough for the accumulation method. They combined the eddy-accumulation method (EA) according to Eq. (4.75) with the flux-variance similarity according to Eq. (2.97). Their method becomes an indirect method:

$$\overline{w'c'} = b\sigma_w(\overline{c^+} - \overline{c^-}) \tag{4.76}$$

where the coefficient $b = 0.627$ for an ideal Gaussian frequency distribution (Wyngaard and Moeng 1992), otherwise low variations occur which are also probably different for different gases (Businger and Oncley 1990; Oncley et al. 1993; Pattey et al. 1993):

$$b = \frac{r_{wc}\sigma_c}{(\overline{c^+} - \overline{c^-})} = 0.6 \pm 0.06 \tag{4.77}$$

The coefficient b is to a large extent independent of the stratification. This is probably due to the opposite stability dependency of the integral turbulence characteristics for the vertical wind and matter (Foken et al. 1995). The relaxed eddy-accumulation (REA) method is schematically shown in Fig. 4.11. The weighting of the concentrations is no longer necessary, but the high switching frequency of the valves for zero passages of the vertical wind is still necessary.

A further improvement was realized with the modified relaxed eddy-accumulation method (MREA) according to Businger and Oncley (1990), which is of practical use and generally called REA. In this method, the air in the case of positive and negative maximal values of the vertical wind velocity are collected into two separate reservoirs; for fluctuations around zero the air is rejected or collected in a control volume (Fig. 4.12).

Equations (4.76) and (4.77) get the following modifications

$$\overline{w'c'} = b\sigma_w\left(\overline{c^+(w > w_0)} - \overline{c^-(w < -w_0)}\right) \tag{4.78}$$

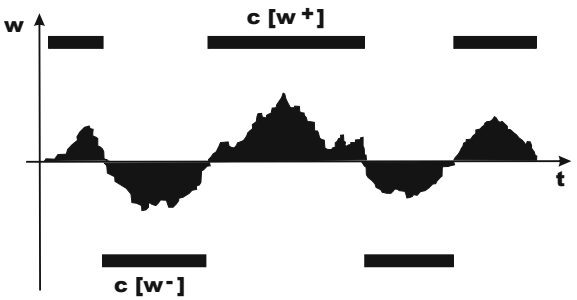

Fig. 4.11 Schematic view of the relaxed eddy-accumulation method (Adapted from Foken et al. 1995, with kind permission of © Gebr. Borntraeger Verlagsgesellschaft Stuttgart 1995, www.schweizerbart.de, All rights reserved)

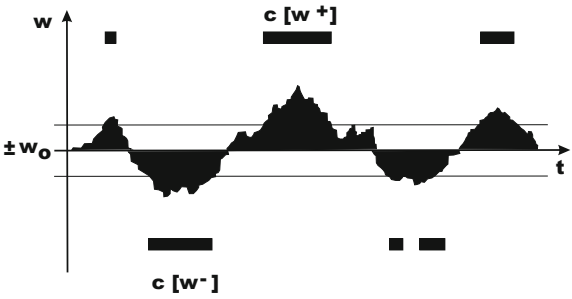

Fig. 4.12 Schematic view of the modified relaxed eddy-accumulation method (Adapted from Foken et al. 1995, with kind permission of © Gebr. Borntraeger Verlagsgesellschaft Stuttgart 1995, www.schweizerbart.de, All rights reserved)

with

$$\frac{b(w_0/\sigma_w)}{b(0)} = e^{-\frac{3}{4}w_0/\sigma_w} \pm 0.012. \tag{4.79}$$

The threshold value w_0 depends on the experimental conditions and the sampled gas. Thus, the parameter b must be updated using a parallel simulation with a proxy parameter, e.g. the temperature or the water vapour:

$$b = \frac{\overline{w'c'_{proxy}}}{\sigma_w\left(\overline{c^{+}_{proxy}(w > w_0)} - \overline{c^{-}_{proxy}(w < -w_0)}\right)} \tag{4.80}$$

Simulation experiments have shown (Ruppert et al. 2006a) that the optimal value for b is approximately 0.6. The accuracy of the method is up to one order lower if a constant b-value is used as compared to the determination with a proxy value. It must be taken into consideration that scalars act similar only for small eddies (Pearson et al. 1998). This is not the case for the application of larger eddies (Ruppert et al. 2006a). This so-called scalar similarity can also change during the daily cycle (see also Sect. 3.5.5). Therefore the choice of the proxy scalar must be made very carefully. The method fails for low fluxes, which are not only caused by the daily cycle but also the ecosystem. For instance, this is the case about two weeks after the mowing of a meadow (Riederer et al. 2014).

For the implementation of the method, the measurement system must be adapted to the streamlines by a coordinate transformation, and the planar-fit method (Wilczak et al. 2001) is recommended (see Sect. 4.2.3.2). Furthermore attention must be paid so that the integral turbulence characteristics of the vertical wind velocity, which must follow the known dependencies, are not specifically modified by the measurement site. An overall evaluation is given in Table 4.18.

Often, the accuracy of gas analyzers is not high enough to accurately detect concentration differences between both reservoirs. This can be overcome by the hyperbolic relaxed eddy-accumulation method (HREA), which is based on an idea by Shaw (1985). Bowling et al. (1999) and Wichura et al. (2000) expanded this method for operational applications for carbon dioxide isotope fluxes. In this

Table 4.18 Evaluation of the relaxed eddy accumulation method (REA)

Criterion	Evaluation
Area of application	Basic research and extravagant continuous measurement programs
Financial expense	10–50 k€ per system
Personal expense	Continuous scientific and technical support
Education	Good micrometeorological and measurement technique and probably also chemical knowledge
Error	Depending on the micrometeorological conditions 5–20%
Sampling	10–20 Hz
Time resolution of fluxes	30–60 min
Application for chemical compounds	Selected inert gases (gas analysers with high time resolution)
Restrictions in the application	Sufficient footprint area, turbulent conditions necessary, similarity of turbulent scales of the scalars, no local influences on integral turbulence characteristics

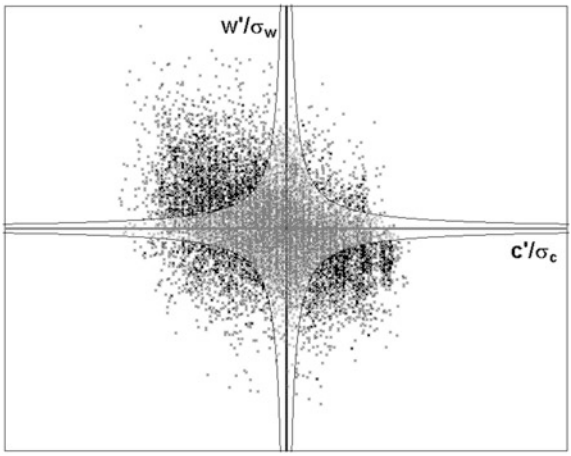

Fig. 4.13 Schematic view of the hyperbolic relaxed eddy-accumulation method (Adapted from Ruppert et al. 2002, with kind permission of © Authors 2002, All rights reserved)

method, only air is collected outside a hyperbolic curve, which must be defined for each particular study (Fig. 4.13)

$$\left|\frac{w'}{\sigma_w}\frac{c'}{\sigma_c}\right| > D \quad \text{for w} > 0, \tag{4.81}$$

$$\left|\frac{w'}{\sigma_w}\frac{c'}{\sigma_c}\right| > D \quad \text{for w} < 0. \tag{4.82}$$

The hyperbolic relaxed eddy-accumulation method requires considerable efforts to accurately determine the dead band. The value calculated by Bowling et al. (1999) $D = 1.1$ is probably too large so that only extreme events are collected

Table 4.19 Evaluation of the hyperbolic relaxed eddy accumulation method (HREA)

Criterion	Evaluation
Area of application	Basic research
Financial expense	10–50 k€ per system
Personal expense	Intensive scientific and technical support
Education	Good micrometeorological and measurement technique and probably also chemical knowledge
Error	Depending on the micrometeorological conditions 5–20%
Sampling	10–20 Hz
Time resolution of fluxes	30–60 min
Application for chemical compounds	Selected inert gases (gas analysers with high time resolution)
Restrictions in the application	Sufficient footprint area, turbulent conditions necessary, similarity of turbulent scales of the scalars, no local influences on integral turbulence characteristics

which are not adequately distributed among the quadrants. A simulation study by Ruppert et al. (2006a) showed that an optimal value is $D \sim 0.8$. An adequate choice of the proxy scalar and the control of the scalar similarity of the measured quantity and proxy parameters are very important. Deviations have a much larger effect than in the case of the simple REA method.

The benefit of the hyperbolic relaxed eddy-accumulation method, the significant increase of the concentration differences in both reservoirs, may be compensated by the high standards needed for turbulent similarity relations being applicable. An overall evaluation is given in Table 4.19.

Besides improved analyzers for trace gases, which allows the application of the eddy-covariance method (see Sect. 4.2) or at least of the disjunct eddy-covariance method (see Sect. 4.4.3), there are still single REA applications such as for nitrous acid (HONO, Ren et al. 2011), peroxyacetyl nitrate (PAN, Moravek et al. 2014) or ^{13}C isotopes (Riederer et al. 2014). Because these systems need longer suction tubes, the triggering of the valves based on the vertical wind velocity must be highly accurate and timed correctly (Moravek et al. 2013).

4.4.3 Disjunct Eddy-Covariance Method (DEC)

Up to now, only methods have been discussed which can be used for inert gases or gases that do not react during their stay in the reservoirs. Gas analyzers with sampling rates of about 10–20 Hz are necessary for the measurement of turbulent fluxes with the eddy-covariance method. Such instruments are available for only a few gases such as ozone. The basic idea of the disjunct eddy-covariance method borrows from the eddy-covariance method for aircraft measurements and is therefore a direct measurement method. Due to the velocity of the aircraft and the

Table 4.20 Evaluation of the disjunct eddy-covariance method (DEC)

Criterion	Evaluation
Area of application	Basic research
Financial expense	10–100 k€ per system
Personal expense	Intensive continuous scientific and technical support
Education	Good micrometeorological, measurement technique and chemical knowledge
Error	Depending on the micrometeorological conditions 5–20%
Sampling	1–30 s, sampling duration <0.1 s
Time resolution of fluxes	30–60 min
Application for chemical compounds	Selected inert gases (gas analysers with time resolution <30 s)
Restrictions in the application	Sufficient footprint area, turbulent conditions necessary

nearly identical sampling frequencies as for surface measurements, the sampling frequency cannot be optimized according to the sampling theorem (see Sect. 6.1.2) to resolve the turbulent eddies. According to investigations by Lenschow et al. (1994), it is possible to estimate fluxes for a fully-developed turbulent regime even when the sampling frequency is low in comparison to the eddy size. This means a larger separation in time (disjunct) of the single samples.

This is the benefit of the disjunct eddy-covariance method where samples are taken only in certain time intervals. Although the direct sampling is taken over a time interval <0.1 s, it may take the gas analyzer several seconds to record the data due to its high inertia, assuming no remarkable reactions occur during this time. Based on simulations, the time difference between two samplings should be in the range of 1–30 s to get the errors comparable to the eddy-covariance method. The method was successfully applied several times (Rinne et al. 2000; Ammann et al. 2006; Held et al. 2007; Schmidt and Klemm 2008; Turnipseed et al. 2009), amongst others with mass spectrometers for reactive gases and aerosols. An overview of the method was given by Rinne and Ammann (2012) and an evaluation of the method is given in Table 4.20.

4.4.4 Surface Renewal Method

The surface renewal method (Paw U et al. 1995) is based on the concept of eddy accumulation (conditional sampling). Instead of turbulence measurements, ramp structures in concentration time series over the vegetation are detected of (see Sect. 3.5.2). Due to the constant *renewal* of these structures, the flux can be defined based on storage depletion. The concept was derived for the sensible heat flux but it can also be applied for matter fluxes. The sensible heat flux is defined as the

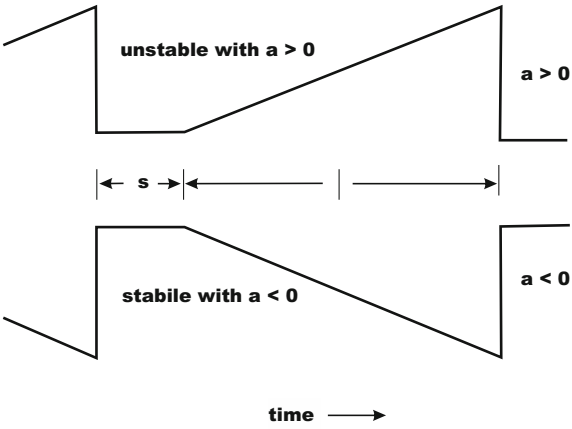

Fig. 4.14 Schematic view of the calculation of ramp structures of the surface renewal method (Adapted from Snyder et al. 1996, with kind permission of © Kluwer Academic Publisher B. V. Dordrecht 1996, All rights reserved)

temperature change in time in a volume V above an area A, where V/A can be used as canopy height z_B:

$$Q_H = \rho\, c_p \frac{dT}{dt}\left(\frac{V}{A}\right) \tag{4.83}$$

Ramp structures such as those shown in Fig. 4.14 for stable and unstable stratification form the basis (Paw U et al. 1995; Snyder et al. 1996). Accordingly, the temperature change in time dT/dt in Eq. (4.83) can be substituted by a/l and is multiplied with the relative duration of the heating or cooling $l/(l + s)$:

$$Q_H = \rho\, c_p \frac{a}{l+s} z_B \tag{4.84}$$

The method needs careful analysis of the turbulence structure and promises possibilities for the application of fluxes above high vegetation, especially for predominant stabile stratification with significant ramp structures. There are only a few experimental studies available (Katul et al. 1996; Snyder et al. 1996; Castellví and Snyder 2010; Castellví et al. 2012). An evaluation is given in Table 4.21.

4.5 Fluxes of Chemical Substances

The deposition of chemical substances occurs in three different ways (Foken et al. 1995; Finlayson-Pitts and Pitts 2000):

- wet deposition of solute gases and substances in rain water,
- moist deposition of solute gases and substances in fog water,
- dry deposition by turbulent transport of gases and particles (aerosols).

Table 4.21 Evaluation of the surface renewal method

Criterion	Evaluation
Area of application	Basic research and extensive continuous measurement programs for special cases
Financial expense	5–10 k€ per system
Personal expense	Intensive continuous scientific and technical support
Education	Good micrometeorological and measurement technique and probably also chemical knowledge
Error	Depending on the micrometeorological conditions 10–30%
Sampling	10–20 Hz
Time resolution of fluxes	30–60 min
Application for chemical compounds	Selected inert gases (gas analysers with high time resolution)
Restrictions in the application	Sufficient footprint area, turbulent conditions necessary, only over vegetation with ramp structures

Only the dry deposition can be measured with the previously described methods of energy and matter exchange. The wet deposition is a precipitation measurement made with so-called wet-only collectors, which open only during precipitation to avoid the collection of dry deposition and sedimentation. The problems with this measurement are similar to those for precipitation measurement (see Sect. 6.2.4). The moist deposition is important only in areas with frequent fog conditions such as hilly regions (Wrzesinsky and Klemm 2000).

In ecological studies, bulk deposition is measured with open collectors located in the trunk space of a forest. These measurements are the sums of the wet deposition, the sedimentation, the wash up of deposited substances from leafs, and partly dry deposition. The crown-eaves method attempts to compare the bulk deposition with the wet deposition outside the forest, and to estimate the dry deposition as a difference term (Guderian 2000). This method cannot measure the dry deposition quantitatively, because substances are also directly absorbed by the plant surfaces or deposited in the under story or the soil. Also, the sampling time cannot be equated with the time of deposition.

The distribution of the total deposition of the three deposition paths depends significantly on the properties of the surface. High vegetation with a large surface roughness more efficiently absorbs matter by dry deposition from the air (comb out) than by wet or moist deposition. Depending on the substances, dry deposition makes a contribution to the total deposition of about 3/4 above high vegetation and 2/3 above low vegetation (Foken et al. 1995). The substance-dependent differences are shown in Table 4.22.

The dry deposition can be determined, in principle, with all the methods described thus far. One of the difficulties is the limited number of gases for which high-frequency gas analyzers are available for the eddy-covariance method. For profile measurements, the absolute accuracy of the gas analyzers is often too poor to provide for the necessary resolution or the sampling times are larger than the typical

Table 4.22 Ratio of the dry deposition (TD) to the wet deposition (WD) resp. dry particle deposition (TPD) over rural areas (Foken et al. 1995)

Matter	High roughness (forest)		Low roughness (meadow)	
SO_2/SO_4^-	3–4:1 1:1	TD/WD TD/TPD	1–1.5:1 3–10:1	TD/WD TD/TPD
$NO_2 + HNO_3$	1.8–4:1	TD/WD	1–2:1	TD/WD
NO_3^-	1.2–2:1	TD/TPD	2–10:1	TD/TPD
NH_3/NH_4^+	0.2–5:1 0.2–5:1	TD/WD TD/TPD	? 1:1	TD/WD TD/TPD
metal	~1:1	TD/WD	1:20	TD/WD

meteorological averaging times. Often, modified Bowen-ratio methods, flux-variance similarities, or accumulation methods are utilized. All these methods are not suitable for continuous, operational measurement programs. For recording of the dry deposition estimates, the so-called deposition velocity is used. For climate research worldwide, carbon dioxide exchange is measured with the eddy-covariance method within the FLUXNET programme (Baldocchi et al. 2001). Therefore, extensive technical guides are available (Moncrieff et al. 1997; Aubinet et al. 2000, 2003b, 2012a). Recently efforts have been made to standardize measurement and analysis methods within larger national (NEON, SanClements et al. 2014) and international (ICOS) programs. However, limitations exist due to the variability of atmospheric turbulence and the adaption of instruments and models.

All mentioned methods are unsuitable for routine measurements. A simple and routinely applicable, but physically unrealistic, method is based on the deposition velocity defined by Chamberlain (1961):

$$v_D(z) = -\frac{Q_c}{c(z)} \tag{4.85}$$

This definition is inconsistent with the gradient approach (Roth 1975). But the deposition velocity can be assumed to be a reciprocal transport resistance (see Sect. 5.3), in which the concentration can be replaced by the concentration difference between the measurement height and a second reference height (in the ground), where the concentration is constant or very low. In this way, the physical incorrectness can be overcome. This assumption has the disadvantage that short time changes of the dry deposition (daily cycle or shorter) cannot be exactly reproduced. The method is therefore only applicable for long-term measurements.

Deposition velocities are on the order of 10^{-3} m s^{-1} and are highly variable depending on the surface and the meteorological conditions (Table 4.23). For countrywide investigations, the deposition velocity listed by the relevant agencies is dependent on the time of the year in which the averaged dry deposition was measured.

The proportionality given in Eq. (4.85) between the flux and the concentration is generally fulfilled only for unstable and neutral stratification. Figure 4.15 shows

Table 4.23 Examples for the deposition velocity (Helbig et al. 1999)

Gas	Surface	v_D in 10^{-2} m s^{-1}	Conditions
SO_2	Grass	0.5	Neutral stratification
	Needle forest	0.3–0.6	Averaged value
O_3	Grass	0.55	Neutral, 5 m s^{-1}
	Spruce forest	0.4	Averaged value
NO	Grass	0.05	Neutral, 5 m s^{-1}
	Spruce forest	0.1–0.4	Averaged value
NO_2	Grass	0.6	Neutral, 5 m s^{-1}
	Spruce forest	1.2	In spring

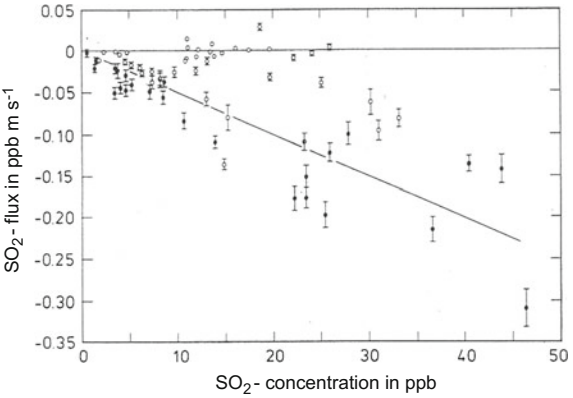

Fig. 4.15 Dependency of the sulphur dioxide deposition on the concentration under the assumption of a constant deposition velocity; filled symbols are values at noon time with unstable stratification, and open symbols values with stable stratification (Adapted from Hicks and Matt 1988, with kind permission of © Kluwer Academic Publisher B. V. Dordrecht 1988, All rights reserved)

that this proportionality can be realized only with a large scatter. For stable stratification, changes of the concentration are nearly independent of the flux.

Due to the non-physical definition of the deposition velocity, there are also problems with its experimental determination. The exact definition would be the transport or transfer velocity (Roth 1975; Arya 1999):

$$v_D(z) = -\frac{Q_c}{c(z) - c(0)} \tag{4.86}$$

Only for the case $c(0) = 0$, i.e. for matter which disappears nearly completely by reactions at the surface, the deposition velocity would be identical with the transfer velocity. Otherwise one obtains unrealistic values (Businger 1986). The determination of the transfer velocity can be made with all the methods described in this chapter; however, the profile method (see Sect. 4.1) is the simplest method.

Most common is the determination of the deposition velocity with the resistance approach (Seinfeld and Pandis 1998), which is described in detail in Sect. 5.3. Thus, the calculation using simple models is possible (Hicks et al. 1987). An evaluation of the method with the deposition velocity is given in Table 4.24.

Table 4.24 Evaluation of the determination of the dry deposition with the deposition velocity

Criterion	Evaluation
Area of application	Operational measurement programs
Financial expense	2–15 k€ per system
Personal expense	Technical support
Education	Knowledge in measurement technique
Error	According to the micrometeorological conditions 20–50%, partly >50%
Sampling	1–10 s, determination of averages over 10–30 min
Time resolution of fluxes	Decadal and monthly averages
Application for chemical compounds	Selected inert gases
Restrictions in the application	Only for rough estimates usable

The previous remarks are only valid for inert gases like carbon dioxide or sulphur dioxide. For reactive gases, the methods can be used only if one gas is significantly in surplus or the measurement time is significantly shorter than the reaction time (e.g. application of the disjunct eddy-covariance method) and reactions do not play an important role, for example ozone deposition during daytime in a rural area. It is also possible to combine complexes of matter, for instance the NO_x-triade consisting of nitrogen monoxide, nitrogen dioxide, and ozone, or the ammonium-tirade consisting of ammoniac, ammonium ions and ammonium nitrate. With the application of the profile method, it must be taken into account that due to reactions the gradient does not always represent the direction of the flux (Kramm et al. 1996). For the application of the eddy-covariance and eddy-accumulation methods, it must be considered that the reaction times of typical chemical reactions are in the order of 10^1–10^4 s and therefore just in the range of the turbulence fluctuations (Fig. 4.16). Very critical are the conditions of stable stratification. Therefore, these methods are basically unusable except if turbulent eddies are tracked with multipoint measurements under the assumption of isotropic turbulence (Foken et al. 1995).

A measure for the ratio of the transport time to the reaction time is the Damköhler number (Molemaker and Vilà-Guerau de Arellano 1998)

$$Da_t = \frac{t_d}{t_c} k \langle c^* \rangle, \tag{4.87}$$

where k is the kinematic reaction constant and $\langle c^* \rangle$ is a dimensionless volume-averaged concentration of one of the reaction partners in equilibrium. Other definitions scale with the emission flux (Schumann 1989). Because the reactions often occur within the smallest eddies, the Kolmogorov-Damköhler number is applied

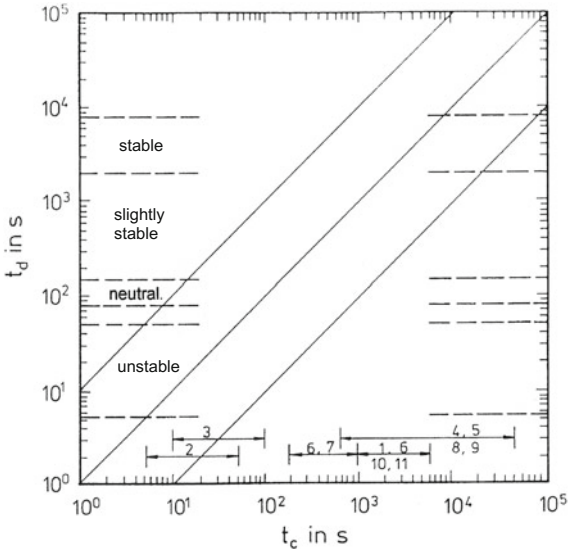

Fig. 4.16 Relation between the characteristic transport time t_d and characteristic reaction time t_c for different chemical reactions for a layer of 10 m thickness and different thermal stratifications according to Dlugi (1993), 1: $HO_2 + HO_2 \rightarrow H_2O_2 + O_2$, 2: $HNO_3 + NH_3 \leftrightarrow NH_4NO_3$, 3: $O_3 + NO \rightarrow NO_2 + O_2$, 4: O_3 + isoprene → reaction products (R), 5: O_3 + monoisoprene → R, 6: NO_3 + monoisoprene → R, 7: NO_3 + isoprene → R, 8: OH + isoprene → R, 9: OH + monoisoprene → R, 10: O_3 + olefins → R, 11: $O_3 + NO_2 \rightarrow NO_3 + O_2$ (Published with kind permission of © SPB Academic Publisher, The Hague 1993, All rights reserved)

$$Da_k = \sqrt{\frac{v}{\varepsilon}} k \langle c^* \rangle \tag{4.88}$$

with the kinematic viscosity, υ, and the energy dissipation ε. An estimate of the dependence of chemical reactions on the Damköhler number was given by Bilger (1980):

$$\begin{array}{ll} Da_t \ll 1 & \text{slow chemistry} \\ Da_k < 1 < Da_t & \text{moderate chemistry} \\ Da_k \gg 1 & \text{fast chemistry} \end{array} \tag{4.89}$$

The determination of the exact transfer and reaction times is important. For the transfer times the method by Vilà-Guerau de Arellano and Duynkerke (1992) is widely applied:

$$t_d = \frac{\kappa \cdot (z + z_0)}{\frac{\sigma_w^2}{u_*^2} \cdot u_*} \tag{4.90}$$

Often the value for σ_w^2/u_*^2 is parametrized using a value of 1.6 according Eq. (2.102). Consequently, Eq. (4.90) is then only valid for neutral stratification (Wyngaard 1982). An estimate for single layers in the surface layer by considering of the stratification based on Eq. (2.75) was given by Mayer et al. (2011):

$$t_d = \frac{\Delta z^2 \cdot \varphi_H(\varsigma) \cdot Sc_t}{\kappa \cdot z_m \cdot u_*}. \tag{4.91}$$

The reaction time, e.g. for the reaction of ozone and nitrogen monoxide with the reaction rate k by Atkinson et al. (2004)

$$O_3 + NO \xrightarrow{k} NO_2 + O_2, k = 1.40 \cdot 10^{-12} exp\left(\frac{-1310}{T}\right), \tag{4.92}$$

according to Lenschow (1982) is given by

$$t_c = \frac{2}{\sqrt{j_{NO_2} + k^2(N_{O_3} + N_{NO})^2 + 2k j_{NO_2}(N_{O_3} + N_{NO} + 2N_{NO_2})}} \tag{4.93}$$

with the photolysis rate for NO_2 (j_{NO_2}) and the molecule density N in mol cm^{-3}.

Vilà-Guerau de Arellano (2003) explicitly recommended that chemical reactions and turbulent transport are always being considered together and that the determination of the Damköhler number is of vital importance. Foken et al. (2012a), among others, confirmed this for the matter exchange in high vegetation, where the diurnal cycle of the Damköhler number was found being highly variable.

References

Akima H (1970) A new method of interpolation and smooth curve fitting based on local procedures. J Assc Comp Mach. 17:589–602.

Ammann C, Brunner A, Spirig C and Neftel A (2006) Technical note: Water vapour concentration and flux measurements with PTR-MS. Atmos Chem Phys. 6:4643–4651.

Arya SP (1999) Air Pollution Meteorology and Dispersion. Oxford University Press, New York, Oxford, 310 pp.

Arya SP (2001) Introduction to Micrometeorology. Academic Press, San Diego, 415 pp.

Atkinson R, Baulch DL, Cox RA, Crowley JN, Hampson RF, Hynes RG, Jenkin ME, Rossi MJ and Troe J (2004) Evaluated kinetic and photochemical data for atmospheric chemistry: Volume I - gas phase reactions of O_x, HO_x, NO_x and SO_x species. Atmos Chem Phys. 4:1461–1738.

Aubinet M, Grelle A, Ibrom A, Rannik Ü, Moncrieff J, Foken T, Kowalski AS, Martin PH, Berbigier P, Bernhofer C, Clement R, Elbers J, Granier A, Grünwald T, Morgenstern K, Pilegaard K, Rebmann C, Snijders W, Valentini R and Vesala T (2000) Estimates of the annual net carbon and water exchange of forests: The EUROFLUX methodology. Adv Ecol Res. 30:113–175.

Aubinet M, Heinesch B and Yernaux M (2003a) Horizontal and vertical CO_2 advection in a sloping forest. Boundary-Layer Meteorol. 108:397–417.

Aubinet M, Clement R, Elbers J, Foken T, Grelle A, Ibrom A, Moncrieff H, Pilegaard K, Rannik U and Rebmann C (2003b) Methodology for data acquisition, storage and treatment. In: Valentini R (ed.), Fluxes of Carbon, Water and Energy of European Forests. Ecological Studies, Vol. 163. Springer, Berlin, Heidelberg, 9–35.

Aubinet M, Berbigier P, Bernhofer C, Cescatti A, Feigenwinter C, Granier A, Grünwald T, Havrankova K, Heinesch B, Longdoz B, Marcolla B, Montagnani L and Sedlak P (2005) Comparing CO_2 storage and advection conditions at night at different CarboEuroflux sites. Boundary-Layer Meteorol. 116:63–94.

Aubinet M, Feigenwinter C, Heinesch B, Bernhofer C, Canepa E, Lindroth A, Montagnani L, Rebmann C, Sedlak P and van Gorsel E (2010) Direct advection measurements do not help to solve the night-time CO_2 closure problem: Evidence from three different forests. Agrical Forest Meteorol. 150:655–664.

Aubinet M, Vesala T and Papale D (eds) (2012a) Eddy Covariance: A Practical Guide to Measurement and Data Analysis. Springer, Dordrecht, Heidelberg, London, New York, 438 pp.

Aubinet M, Feigenwinter C, Heinesch B, Laffineur Q, Papale D, Reichstein M, Rinne J and Van Gorsel E (2012b) Nighttime flux correction. In: Aubinet Met al (eds.), Eddy Covariance: A Practical Guide to Measurement and Data Analysis. Springer, Berlin, Heidelberg, 133–157.

Baldocchi D, Falge E, Gu L, Olson R, Hollinger D, Running S, Anthoni P, Bernhofer C, Davis K, Evans R, Fuentes J, Goldstein A, Katul G, Law B, Lee XH, Malhi Y, Meyers T, Munger W, Oechel W, PawU KT, Pilegaard K, Schmid HP, Valentini R, Verma S and Vesala T (2001) FLUXNET: A new tool to study the temporal and spatial variability of ecosystem-scale carbon dioxide, water vapor, and energy flux densities. Bull Amer Meteorol Soc. 82:2415–2434.

Barr AG, King KM, Gillespie TJ, Hartog GD and Neumann HH (1994) A comparison of Bowen ratio and eddy correlation sensible and latent heat flux measurements above deciduous forest. Boundary-Layer Meteorol. 71:21–41.

Bartels J (1935) Zur Morphologie geophysikalischer Zeitfunktionen. Sitzungsberichte Preuß Akad Wiss. 30:504–522.

Barthlott C and Fiedler F (2003) Turbulence structure in the wake region of a meteorological tower. Boundary-Layer Meteorol. 108:175–190.

Bernhardt K and Piazena H (1988) Zum Einfluß turbulenzbedingter Dichteschwankungen auf die Bestimmung turbulenter Austauschströme in der Bodenschicht. Z Meteorol. 38:234–245.

Bernhofer C (1992) Estimating forest evapotranspiration at a non-ideal site. Agrical Forest Meteorol. 60:17–32.

Bilger RW (1980) Turbulent flows with nonpremixed reactants. In: Libby PA and Willimas FA (eds.), Turbulent Reacting Flows. Springer, Berlin, Heidelberg, 65–113.

Bowling DR, Delany AC, Turnispseed AA, Baldocchi DD and Monson RK (1999) Modification of the relaxed eddy accumulation technique to maximize measured scalar mixing ratio differences in updrafts and downdrafts. J Geophys Res. 104:9121–9133.

Bowling DR, Pataki DE and Ehleringer JR (2003) Critical evaluation of micrometeorological methods for measuring ecosystem-atmosphere isotopic exchange of CO_2. Agrical Forest Meteorol. 116:159–179.

Brocks K and Krügermeyer L (1970) Die hydrodynamische Rauhigkeit der Meeresoberfläche. Ber Inst Radiometeorol Marit Meteorol. 14:55 pp.

Brook RR (1978) The influence of water vapor fluctuations on turbulent fluxes. Boundary-Layer Meteorol. 15:481–487.

Burba G, McDermitt DK, Grelle A, Anderson DJ and Xu L (2008) Addressing the influence of instrument surface heat exchange on the measurements of CO2 flux from open-path gas analyzers. Global Change Biology. 14:1854–1876.

Businger JA (1986) Evaluation of the accuracy with which dry deposition can be measured with current micrometeorological techniques. J Appl Meteorol. 25:1100–1124.

Businger JA and Oncley SP (1990) Flux measurement with conditional sampling. J Atm Oceanic Techn. 7:349–352.
Castellví F and Snyder RL (2010) A comparison between latent heat fluxes over grass using a weighing lysimeter and surface renewal analysis. J Hydrol. 381:213–220.
Castellví F, Consoli S and Papa R (2012) Sensible heat flux estimates using two different methods based on surface renewal analysis. A study case over an orange orchard in Sicily. Agrical Forest Meteorol. 152:58–64.
Chamberlain AC (1961) Aspects of travel and deposition of aerosol and vapour clouds. A.E.R.E., Harwell, Berkshire, 38 pp.
Charuchittipan D, Babel W, Mauder M, Leps J-P and Foken T (2014) Extension of the averaging time of the eddy-covariance measurement and its effect on the energy balance closure Boundary-Layer Meteorol. 152:303–327.
Desjardins RL (1977) Description and evaluation of a sensible heat flux detector. Boundary-Layer Meteorol. 11:147–154.
Desjardins RL, MacPherson JI, Schuepp PH and Karanja F (1989) An evaluation of aircraft flux measurements of CO_2, water vapor and sensible heat. Boundary-Layer Meteorol. 47:55–69.
Dlugi R (1993) Interaction of NO_x and VOC's within vegetation. In: Borrell PW (ed.), Proceedings EUROTRAC-Symposium 92. SPB Acad. Publ., The Hague, 682–688.
Doran JC and Verholek MG (1978) A note on vertical extrapolation formulas for Weibull velocity distribution parameters. J Climate Appl Meteorol. 17:410–412.
Dugas WA, Fritschen LJ, Gay LW, Held AA, Matthias AD, Reicosky DC, Steduto P and Steiner JL (1991) Bowen ratio, eddy correlation, and portable chamber measurements of sensible and latent heat flux over irrigated spring wheat. Agrical Forest Meteorol. 56:12–20.
Dyer AJ (1974) A review of flux-profile-relationships. Boundary-Layer Meteorol. 7:363–372.
Dyer AJ (1981) Flow distortion by supporting structures. Boundary-Layer Meteorol. 20:363–372.
Eugster W and Senn W (1995) A cospectral correction for measurement of turbulent NO_2 flux. Boundary-Layer Meteorol. 74:321–340.
Falge E, Baldocchi D, Olson R, Anthoni P, Aubinet M, Bernhofer C, Burba G, Ceulemans R, Clement R, Dolman H, Granier A, Gross P, Grunwald T, Hollinger D, Jensen NO, Katul G, Keronen P, Kowalski A, Lai CT, Law BE, Meyers T, Moncrieff H, Moors E, Munger JW, Pilegaard K, Rannik U, Rebmann C, Suyker A, Tenhunen J, Tu K, Verma S, Vesala T, Wilson K and Wofsy S (2001) Gap filling strategies for long term energy flux data sets. Agrical Forest Meteorol. 107:71–77.
Finkelstein PL and Sims PF (2001) Sampling error in eddy correlation flux measurements. J Geophys Res. D106:3503–3509.
Finlayson-Pitts BJ and Pitts JN (2000) Chemistry of the Upper and Lower Atmosphere. Academic Press, San Diego, 963 pp.
Finnigan J (1999) A comment on the paper by Lee (1998): "On micrometeorological observations of surface-air exchange over tall vegetation". Agrical Forest Meteorol. 97:55–64.
Finnigan JJ, Clement R, Malhi Y, Leuning R and Cleugh HA (2003) A re-evaluation of long-term flux measurement techniques, Part I: Averaging and coordinate rotation. Boundary-Layer Meteorol. 107:1–48.
Foken T (1990) Turbulenter Energieaustausch zwischen Atmosphäre und Unterlage - Methoden, meßtechnische Realisierung sowie ihre Grenzen und Anwendungsmöglichkeiten. Ber Dt Wetterdienstes. 180:287 pp.
Foken T (1998) Genauigkeit meteorologischer Messungen zur Bestimmung des Energie- und Stoffaustausches über hohen Pflanzenbeständen. Ann Meteorol. 37:513–514.
Foken T and Skeib G (1980) Genauigkeit und Auswertung von Profilmessungen zur Energieaustauschbestimmung. Z Meteorol. 30:346–360.
Foken T and Oncley SP (1995) Results of the workshop 'Instrumental and methodical problems of land surface flux measurements'. Bull Amer Meteorol Soc. 76:1191–1193.
Foken T and Wichura B (1996) Tools for quality assessment of surface-based flux measurements. Agrical Forest Meteorol. 78:83–105.

Foken T, Dlugi R and Kramm G (1995) On the determination of dry deposition and emission of gaseous compounds at the biosphere-atmosphere interface. Meteorol Z. 4:91–118.
Foken T, Richter SH and Müller H (1997a) Zur Genauigkeit der Bowen-Ratio-Methode. Wetter und Leben. 49:57–77.
Foken T, Jegede OO, Weisensee U, Richter SH, Handorf D, Görsdorf U, Vogel G, Schubert U, Kirzel H-J and Thiermann V (1997b) Results of the LINEX-96/2 Experiment. Dt Wetterdienst, Forsch. Entwicklung, Arbeitsergebnisse. 48:75 pp.
Foken T, Göckede M, Mauder M, Mahrt L, Amiro BD and Munger JW (2004) Post-field data quality control. In: Lee X et al (eds.), Handbook of Micrometeorology: A Guide for Surface Flux Measurement and Analysis. Kluwer, Dordrecht, 181–208.
Foken T, Wimmer F, Mauder M, Thomas C and Liebethal C (2006) Some aspects of the energy balance closure problem. Atmos Chem Phys. 6:4395–4402.
Foken T, Meixner FX, Falge E, Zetzsch C, Serafimovich A, Bargsten A, Behrendt T, Biermann T, Breuninger C, Dix S, Gerken T, Hunner M, Lehmann-Pape L, Hens K, Jocher G, Kesselmeier J, Lüers J, Mayer JC, Moravek A, Plake D, Riederer M, Rütz F, Scheibe M, Siebicke L, Sörgel M, Staudt K, Trebs I, Tsokankunku A, Welling M, Wolff V and Zhu Z (2012a) Coupling processes and exchange of energy and reactive and non-reactive trace gases at a forest site—results of the EGER experiment. Atmos Chem Phys. 12:1923–1950.
Foken T, Aubinet M and Leuning R (2012b) The eddy-covarianced method. In: Aubinet M et al (eds.), Eddy Covariance: A Practical Guide to Measurement and Data Analysis. Springer, Dordrecht, Heidelberg, London, New York, 1–19.
Foken T, Leuning R, Oncley SP, Mauder M and Aubinet M (2012c) Corrections and data quality In: Aubinet M et al (eds.), Eddy Covariance: A Practical Guide to Measurement and Data Analysis. Springer, Dordrecht, Heidelberg, London, New York, 85–131.
Frank JM, Massman WJ and Ewers BE (2013) Underestimates of sensible heat flux due to vertical velocity measurement errors in non-orthogonal sonic anemometers. Agrical Forest Meteorol. 171–172:72–81.
Fratini G and Mauder M (2014) Towards a consistent eddy-covariance processing: an intercomparison of EddyPro and TK3. Atmos Meas Techn. 7:2273–2281.
Fuchs M and Tanner CB (1970) Error analysis of Bowen ratios measured by differential psychrometry. Agric Meteorol. 7:329–334.
Fuehrer PL and Friehe CA (2002) Flux correction revised. Boundary-Layer Meteorol. 102:415–457.
Garratt JR (1992) The Atmospheric Boundary Layer. Cambridge University Press, Cambridge, 316 pp.
Geernaert GL (ed) (1999) Air-Sea Exchange: Physics, Chemistry and Dynamics. Kluwer Acad. Publ., Dordrecht, 578 pp.
Goulden ML, Munger JW, Fan F-M, Daube BC and Wofsy SC (1996) Measurements of carbon sequestration by long-term eddy covariance: method and critical evaluation of accuracy. Global Change Biol. 2:159–168.
Grelle A and Burba G (2007) Fine-wire thermometer to correct CO_2 fluxes by open-path analyzers for artificial density fluctuations. Agrical Forest Meteorol. 147:48–57.
Gu L, Falge EM, Boden T, Baldocchi DD, Black T, Saleska SR, Sumi T, Verma SB, Vesala T, Wofsy SC and Xu L (2005) Objective threshold determination for nighttime eddy flux filtering. Agrical Forest Meteorol. 128:179–197.
Guderian R (ed) (2000) Handbuch der Umweltveränderungen und Ökotoxikologie, Atmosphäre. Springer, Berlin, Heidelberg, 424, 516 pp.
Gurjanov AE, Zubkovskij SL and Fedorov MM (1984) Mnogokanalnaja avtomatizirovannaja sistema obrabotki signalov na baze EVM (Automatic multi-channel system for signal analysis with electronic data processing). Geod Geophys Veröff, R II. 26:17–20.
Haugen DA (ed) (1973) Workshop on Micrometeorology. Am. Meteorol. Soc., Boston, 392 pp.
Helbig A, Baumüller J and Kerschgens MJ (eds) (1999) Stadtklima und Luftreinhaltung. Springer, Berlin, Heidelberg, 467 pp.

Held A, Niessner R, Bosveld F, Wrzesinsky T and Klemm O (2007) Evaluation and application of an electrical low pressure impactor in disjunct eddy covariance aerosol flux measurements. Aerosol Science and Technology. 41:510–519.
Hesselberg T (1926) Die Gesetze der ausgeglichenen atmosphärischen Bewegungen. Beitr Phys Atm. 12:141–160.
Hicks BB and Matt DR (1988) Combining biology, chemistry and meteorology in modelling and measuring dry deposition. J Atm Chem. 6:117–131.
Hicks BB, Baldocchi DD, Meyers TP, Hosker jr. RP and Matt DR (1987) A preliminary multiple resistance routine for deriving dry deposition velocities from measured quantities. Water, Air and Soil Pollution. 36:311–330.
Hoaglin DC, Mosteller F and Tukey JW (2000) Understanding robust and exploratory data analysis. John Wiley & Sons, New York, 447 pp.
Högström U (1988) Non-dimensional wind and temperature profiles in the atmospheric surface layer: A re-evaluation. Boundary-Layer Meteorol. 42:55–78.
Högström U and Smedman A (2004) Accuracy of sonic anemometers: Laminar wind-tunnel calibrations compared to atmospheric in situ calibrations against a reference instrument. Boundary-Layer Meteorol. 111:33–54.
Højstrup J (1993) A statistical data screening procedure. Meas Sci Techn. 4:153–157.
Hollinger DY and Richardson AD (2005) Uncertainty in eddy covariance measurements and its application to physiological models. Tree Phys. 25:873–885.
Horst TW (1997) A simple formula for attenuation of eddy fluxes measured with first-order-response scalar sensors. Boundary-Layer Meteorol. 82:219–233.
Horst TW, Semmer SR and Maclean G (2015) Correction of a non-orthogonal, three-component sonic aanemometer for flow Distortion by transducer shadowing. Boundary-Layer Meteorol. 155:371–395.
Hsu SA, Meindl EA and Gilhousen DB (1994) Determination of power-law wind-profile exponent under near- neutral stability conditions at sea. J Appl Meteorol. 33:757–765.
Huang CH (1979) A theory of dispersion in turbulent shear flow. Atmos Environm. 13:453–463.
Huges IG and Hase TPA (2010) Measurements and their Uncertainties. Oxford University Press, Oxford, 136 pp.
Hui DF, Wan SQ, Su B, Katul G, Monson R and Luo YQ (2004) Gap-filling missing data in eddy covariance measurements using multiple imputation (MI) for annual estimations. Agrical Forest Meteorol. 121:93–111.
Hyson P, Garratt JR and Francey RJ (1977) Algebraic und elektronic corrections of measured uw covariance in the lower atmosphere. Boundary-Layer Meteorol. 16:43–47.
Ibrom A, Dellwik E, Larsen SE and Pilegaard K (2007a) On the use of the Webb–Pearman–Leuning theory for closed-path eddy correlation measurements. Tellus. B 59:937–946.
Ibrom A, Dellwik E, Flyvbjerg H, Jensen NO and Pilegaard K (2007b) Strong low-pass filtering effects on water vapour flux measurements with closed-path eddy correlation systems. Agrical Forest Meteorol. 147:140–156.
Irvin JS (1978) A theoretical variation of the wind profile power-law exponent as a function of surface roughness and stability. Atmos Environm. 13:191–194.
Itier B (1980) Une méthode simplifièe pour la mesure du flux de chaleur sensible. J Rech Atm. 14:17–34.
Järvi L, Mammarella I, Eugster W, Ibrom A, Siivola E, Dellwik E, Keronen P, Burba G and Vesala T (2009) Comparison of net CO_2 fluxes measured with open- and closed-path infrared gas analyzers in urban complex environment. Boreal Environm Res. 14:499–514.
Joffre SM (1984) Power laws and the empirical representation of velocity and directional sheer. J Climate Appl Meteorol. 23:1196–1203.
Kader BA and Perepelkin VG (1984) Profil skorosti vetra i temperatury v prizemnom sloje atmosfery v uslovijach nejtralnoj i neustojtschivoj stratifikacii (The wind and temperature profile in the near surface layer for neutral and unstable stratification). Izv AN SSSR, Fiz Atm Okeana. 20:151–161.

Kaimal JC (1978) Sonic Anemometer Measurement of Atmospheric Turbulence. In: Hansen B (ed.), Proceedings of the Dynamic Flow Conference 1978 on Dynamic Measurements in Unsteady Flows. Springer Netherlands, 551–565.
Kaimal JC and Gaynor JE (1991) Another look to sonic thermometry. Boundary-Layer Meteorol. 56:401–410.
Kaimal JC and Finnigan JJ (1994) Atmospheric Boundary Layer Flows: Their Structure and Measurement. Oxford University Press, New York, NY, 289 pp.
Kaimal JC, Wyngaard JC, Izumi Y and Coté OR (1972) Spectral characteristics of surface layer turbulence. Quart J Roy Meteorol Soc. 98:563–589.
Kaimal JC, Gaynor JE, Zimmerman HA and Zimmerman GA (1990) Minimizing flow distortion errrors in a sonic anemometer. Boundary-Layer Meteorol. 53:103–115.
Katul G, Hsieh C-I, Oren R, Ellsworth D and Phillips N (1996) Latent and sensible heat flux predictions from a uniform pine forest using surface renewal and flux variance methods. Boundary-Layer Meteorol. 80:249–282.
Kormann R and Meixner FX (2001) An analytical footprint model for non-neutral stratification. Boundary-Layer Meteorol. 99:207–224.
Kowalski A (2006) Comment on "An Alternative Approach for CO2 Flux Correction Caused by Heat and Water Vapour Transfer" by Liu. Boundary-Layer Meteorol. 120:353–355.
Kramm G and Meixner FX (2000) On the dispersion of trace species in the atmospheric boundary layer: a re-formulation of the governing equations for the turbulent flow of the compressible atmosphere. Tellus. 51A:500–522.
Kramm G, Dlugi R and Lenschow DH (1995) A re-evaluation of the Webb correction using density weighted averages. J Hydrol. 166:293–311.
Kramm G, Beier M, Foken T, Müller H, Schröder P and Seiler W (1996) A SVAT-skime for NO, NO_2, and O_3—Model description and test results. Meteorol Atmos Phys. 61:89–106.
Kristensen L, Mann J, Oncley SP and Wyngaard JC (1997) How close is close enough when measuring scalar fluxes with displaced sensors. J Atm Oceanic Techn. 14:814–821.
Lasslop G, Reichstein M, Papale D, Richardson AD, Arneth A, Barr A, Stoy P and Wohlfahrt G (2010) Separation of net ecosystem exchange into assimilation and respiration using a light response curve approach: critical issues and global evaluation. Global Change Biology. 16:187–208.
Lee X (1998) On micrometeorological observations of surface-air exchange over tall vegetation. Agrical Forest Meteorol. 91:39–49.
Lee X, Massman WJ and Law B (eds) (2004) Handbook of Micrometeorology: A Guide for Surface Flux Measurement and Analysis. Kluwer, Dordrecht, 250 pp.
Lege D (1981) Eine Betrachtung zur Bestimmung des Stroms fühlbarer Wärme und der Schubspannungsgeschwindigkeit aus Temperatur- und Windgeschwindigkeitsdifferenzen. Meteorol Rundschau. 34:1–4.
Lenschow DH (1982) Reactive trace species in the boundary layer from a micrometeorological perspective. J Meteor Soc Japan. 60:472–480.
Lenschow DH, Mann J and Kristensen L (1994) How long is long enough when measuring fluxes and other turbulence statistics? J Atm Oceanic Techn. 11:661–673.
Leuning R (2007) The correct form of the Webb, Pearman and Leuning equation for eddy fluxes of trace gases in steady and non-steady state, horizontally homogeneous flows Boundary-Layer Meteorol. 123:263–267.
Leuning R and Legg BJ (1982) Comments on 'The influence of water vapor fluctuations on turbulent fluxes' by Brook. Boundary-Layer Meteorol. 23:255–258.
Leuning R and Judd MJ (1996) The relative merits of open- and closed path analysers for measurements of eddy fluxes. Global Change Biology. 2:241–254.
Liebethal C and Foken T (2003) On the significance of the Webb correction to fluxes. Boundary-Layer Meteorol. 109:99–106.
Liebethal C and Foken T (2004) On the significance of the Webb correction to fluxes, Corrigendum. Boundary-Layer Meteorol. 113:301.

Lindauer M, Schmid HP, Grote R, Mauder M, Steinbrecher R and Wolpert B (2014) Net ecosystem exchange over a non-cleared wind-throw-disturbed upland spruce forest—Measurements and simulations. Agrical Forest Meteorol. 197:219–234.
Liu H (2005) An alternative approach for CO_2 flux correction caused by heat and water vapour transfer. Boundary-Layer Meteorol. 115:151–168.
Liu H and Foken T (2001) A modified Bowen ratio method to determine sensible and latent heat fluxes. Meteorol Z. 10:71–80.
Liu H, Peters G and Foken T (2001) New equations for sonic temperature variance and buoyancy heat flux with an omnidirectional sonic anemometer. Boundary-Layer Meteorol. 100:459–468.
Liu H, Randerson JT, Lindfors J, Massman WJ and Foken T (2006) Consequences of incomplete surface energy balance closure for CO_2 fluxes from open-path CO_2/H_2O infrared gas analyzers. Boundary-Layer Meteorol. 120:65–85.
Lloyd J and Taylor JA (1994) On the temperature dependence of soil respiration. Functional Ecol. 8:315–323.
Mahrt L (1991) Eddy asymmetry in the sheared heated boundary layer. J Atmos Sci. 48:472–492.
Mahrt L (1996) The bulk aerodynamic formulation over heterogeneous surfaces. Boundary-Layer Meteorol. 78:87–119.
Marquardt D (1983) An algorithm for least-sqares estimation of nonlinear parameters. J Soc Indust Appl Math. 11:431–441.
Massman WJ (2000) A simple method for estimating frequency response corrections for eddy covariance systems. Agrical Forest Meteorol. 104:185–198.
Massman WJ and Tuovinen J-P (2006) An analysis and implications of alternative methods of deriving the density (WPL) terms for eddy covariance flux measurements. Boundary-Layer Meteorol. 121:221–227.
Mauder M, Liebethal C, Göckede M, Leps J-P, Beyrich F and Foken T (2006) Processing and quality control of flux data during LITFASS-2003. Boundary-Layer Meteorol. 121:67–88.
Mauder M, Foken T, Clement R, Elbers J, Eugster W, Grünwald T, Heusinkveld B and Kolle O (2008) Quality control of CarboEurope flux data - Part 2: Inter-comparison of eddy-covariance software. Biogeoscience. 5:451–462.
Mauder M, Cuntz M, Drüe C, Graf A, Rebmann C, Schmid HP, Schmidt M and Steinbrecher R (2013) A strategy for quality and uncertainty assessment of long-term eddy-covariance measurements. Agrical Forest Meteorol. 169:122–135.
Mayer JC, Bargsten A, Rummel U, Meixner FX and Foken T (2011) Distributed Modified Bowen Ratio method for surface layer fluxes of reactive and non-reactive trace gases. Agrical Forest Meteorol. 151:655–668.
McMillen RT (1988) An eddy correlation technique with extended applicability to non-simple terrain. Boundary-Layer Meteorol. 43:231–245.
Michaelis L and Menton ML (1913) Die Kinetik der Invertinwirkung. Biochem Z. 49:333.
Moffat AM, Papale D, Reichstein M, Barr AG, Beckstein C, Braswell BH, Churkina G, Desai A, Falge E, Gove JH, Heimann M, Hollinger DY, Hui D, Jarvis AJ, Kattge J, Noormets A, Richardson AD and Stauch VJ (2007) Comprehensive comparison of gap filling techniques for eddy covariance net carbon fluxes. Agrical Forest Meteorol. 47:209–232.
Molemaker MJ and Vilà-Guerau de Arellano J (1998) Control of chemical reactions by convective turbulence in the boundary layer. J Atmos Sci. 55:568–579.
Moncrieff JB, Massheder JM, DeBruin H, Elbers J, Friborg T, Heusinkveld B, Kabat P, Scott S, Søgaard H and Verhoef A (1997) A system to measure surface fluxes of momentum, sensible heat, water vapor and carbon dioxide. J Hydrol. 188–189:589–611.
Moore CJ (1986) Frequency response corrections for eddy correlation systems. Boundary-Layer Meteorol. 37:17–35.
Moravek A, Trebs I and Foken T (2013) Effect of imprecise lag time and high-frequency attenuation on surface-atmosphere exchange fluxes determined with the relaxed eddy accumulation method. J Geophys Res: Atmosph. 118:10, 210–210, 224.

Moravek A, Foken T and Trebs I (2014) Application of a GC-ECD for measurements of biosphere–atmosphere exchange fluxes of peroxyacetyl nitrate using the relaxed eddy accumulation and gradient method. Athmospheric Measurement Techniques. 7:2097–2119.

Müller H, Kramm G, Meixner FX, Fowler D, Dollard GJ and Possanzini M (1993) Determination of HNO_3 dry deposition by modified Bowen ratio and aerodynamic profile techniques. Tellus. 45B:346–367.

Nakai T and Shimoyama K (2012) Ultrasonic anemometer angle of attack errors under turbulent conditions. Agrical Forest Meteorol. 162–163:14–26.

Nakai T, van der Molen MK, Gash JHC and Kodama Y (2006) Correction of sonic anemometer angle of attack errors. Agrical Forest Meteorol. 136:19–30.

Nicholls S and Smith FB (1982) On the definition of the flux of sensible heat. Boundary-Layer Meteorol. 24:121–127.

Nieuwstadt FTM (1978) The computation of the friction velocity u_* and the temperature scale T_* from temperature and wind velocity profiles by least-square method. Boundary-Layer Meteorol. 14:235–246.

Oechel WC, Laskowski CA, Burba G, Gioli B and Kalhori AAM (2014) Annual patterns and budget of CO_2 flux in an Arctic tussock tundra ecosystem. Journal of Geophysical Research: Biogeosciences. 119:2013JG002431.

Ohmura A (1982) Objective criteria for rejecting data for Bowen ratio flux calculations. J Climate Appl Meteorol. 21:595–598.

Oncley SP, Businger JA, Itsweire EC, Friehe CA, LaRue JC and Chang SS (1990) Surface layer profiles and turbulence measurements over uniform land under near-neutral conditions. 9th Symposium on Boundary Layer and Turbulence, Roskilde, Denmark, April 30 - May 3, 1990. Am. Meteorol. Soc., pp. 237–240.

Oncley SP, Delany AC, Horst TW and Tans PP (1993) Verification of flux measurement using relaxed eddy accumulation. Atmos Environm. 27A:2417–2426.

Panin GN (1983) Metodika rastscheta lokalnogo teplo- i vlagoobmena v sisteme vodoem - atmosfera (Method for calculation of local heat and humidity exchange of the system water - atmosphere). Vodnye resursy. 4:3–12.

Papale D and Valentini R (2003) A new assessment of European forests carbon exchanges by eddy fluxes and artificial neural network spatialization. Global Change Biology. 9:525–535.

Papale D, Reichstein M, Aubinet M, Canfora E, Bernhofer C, Kutsch W, Longdoz B, Rambal S, Valentini R, Vesala T and Yakir D (2006) Towards a standardized processing of Net Ecosystem Exchange measured with eddy covariance technique: algorithms and uncertainty estimation. Biogeoscience. 3:571–583.

Pattey E, Desjardins RL and Rochette P (1993) Accuracy of the relaxed eddy accumulation technique. Boundary-Layer Meteorol. 66:341–355.

Pattey E, Strachan IB, Desjardins RL, Edwards GC, Dow D and MacPherson IJ (2006) Application of a tunable diode laser to the measurement of CH_4 and N_2O fluxes from field to landscape scale using several micrometeorological techniques. Agrical Forest Meteorol. 136:222–236.

Paw U KT, Qiu J, Su H-B, Watanabe T and Brunet Y (1995) Surface renewal analysis: a new method to obtain scalar fluxes. Agrical Forest Meteorol. 74:119–137.

Paw U KT, Baldocchi D, Meyers TP and Wilson KB (2000) Correction of eddy covariance measurements incorporating both advective effects and density fluxes. Boundary-Layer Meteorol. 97:487–511.

Pearson jr. RJ, Oncley SP and Delany AC (1998) A scalar similarity study based on surface layer ozone measurements over cotton during the California Ozone Deposition Experiment. J Geophys Res. 103 (D15):18919–18926.

Peterson EW and Hennessey jr. JP (1978) On the use of power laws for estimates of wind power potential. J Climate Appl Meteorol. 17:390–394.

Rannik U and Vesala T (1999) Autoregressive filtering versus linear detrending in estimation of fluxes by the eddy covariance method. Boundary-Layer Meteorol. 91:259–280.

Rebmann C, Göckede M, Foken T, Aubinet M, Aurela M, Berbigier P, Bernhofer C, Buchmann N, Carrara A, Cescatti A, Ceulemans R, Clement R, Elbers J, Granier A, Grünwald T, Guyon D, Havránková K, Heinesch B, Knohl A, Laurila T, Longdoz B, Marcolla B, Markkanen T, Miglietta F, Moncrieff H, Montagnani L, Moors E, Nardino M, Ourcvial J-M, Rambal S, Rannik U, Rotenberg E, Sedlak P, Unterhuber G, Vesala T and Yakir D (2005) Quality analysis applied on eddy covariance measurements at complex forest sites using footprint modelling. Theor Appl Climat. 80:121–141.

Rebmann C, Kolle O, Heinesch B, Queck R, Ibrom A and Aubinet M (2012) Data acquisition and flux calculations. In: Aubinet Met al (eds.), Eddy Covariance: A Practical Guide to Measurement and Data Analysis. Springer, Dordrecht, Heidelberg, London, New York, 59–83.

Reichstein M, Falge E, Baldocchi D, Papale D, Aubinet M, Berbigier P, Bernhofer C, Buchmann N, Gilmanov T, Granier A, Grünwald T, Havránková K, Ilvesniemi H, Janous D, Knohl A, Laurila T, Lohila A, Loustau D, Matteucci G, Meyers T, Miglietta F, Ourcival J-M, Pumpanen J, Rambal S, Rotenberg E, Sanz M, Tenhunen J, Seufert G, Vaccari F, Vesala T, Yakir D and Valentini R (2005) On the separation of net ecosystem exchange into assimilation and ecosystem respiration: review and improved algorithm. Global Change Biology. 11:1424–1439.

Ren X, Sanders JE, Rajendran A, Weber RJ, Goldstein AH, Pusede SE, Browne EC, Min KE and Cohen RC (2011) A relaxed eddy accumulation system for measuring vertical fluxes of nitrous acid. Atmos. Meas. Tech. 4:2093–2103.

Richardson AD, Hollinger DY, Burba GG, Davis KJ, Flanagan LB, Katul GG, Munger JW, Ricciuto DM, Stoy PC, Suyker AE, Verma SB and Wofsy SC (2006) A multi-site analysis of random error in tower-based measurements of carbon and energy fluxes. Agrical Forest Meteorol. 136:1–18.

Richter SH and Skeib G (1984) Anwendung eines Verfahrens zur Parametrisierung des turbulenten Energieaustausches in der atmosphärischen Bodenschicht. Geod Geophys Veröff, R II. 26:80–85.

Richter SH and Skeib G (1991) Ein Verfahren zur Parametrisierung von Austauschprozessen in der bodennahen Luftschicht. Abh Meteorol Dienstes DDR. 146:15–22.

Riederer M, Hübner J, Ruppert J, Brand WA and Foken T (2014) Prerequisites for application of hyperbolic relaxed eddy accumulation on managed grasslands and alternative net ecosystem exchange flux partitioning. Atmos Meas Techn. 7:4237–4250.

Rinne HJI, Delany AC, Greenberg JP and Guenther AB (2000) A true eddy accumulation system for trace gase fluxes using disjunct eddy sampling method. J Geophys Res. 105(D20):24791–24798.

Rinne J and Ammann C (2012) Disjunct eddy covariance method. In: Aubinet Met al (eds.), Eddy Covariance: A Practical Guide to Measurement and Data. Springer, Dordrecht, Heidelberg, London, New York, 291–307.

Roth R (1975) Der vertikale Transport von Luftbeimengungen in der Prandtl-Schicht und die Depositionsgeschwindigkeit. Meteorol Rundschau. 28:65–71.

Ruppert J, Wichura B, Delany AC and Foken T (2002) Eddy sampling methods, A comparison using simulation results. 15th Symposium on Boundary Layer and Turbulence, Wageningen, 15–19 July 2002. Am. Meteorol. Soc., pp. 27–30.

Ruppert J, Thomas C and Foken T (2006a) Scalar similarity for relaxed eddy accumulation methods. Boundary-Layer Meteorol. 120:39–63.

Ruppert J, Mauder M, Thomas C and Lüers J (2006b) Innovative gap-filling strategy for annual sums of CO_2 net ecosystem exchange. Agrical Forest Meteorol. 138:5–18.

SanClements M, Metzger S, Luo H, Pingintha-Durden N, Zulueta RC and Loescher HW (2014) The National Ecological Observatory Network (NEON): Providing free long-term ecological data on a continental scale. iLEAPS newsletter, Special issue on Environmental Research Infrastructures:23–26.

Santoso E and Stull RB (1998) Wind and temperature profiles in the Radix layer: The botton fifth of the convective boundary layer. J Appl Meteorol. 37:545–558.

Schmidt A and Klemm O (2008) Direct determination of highly size-resolved turbulent particle fluxes with the disjunct eddy covariance method and a 12 – stage electrical low pressure impactor. Atmos Chem Phys. 8:7405–7417.

Schotanus P, Nieuwstadt FTM and DeBruin HAR (1983) Temperature measurement with a sonic anemometer and its application to heat and moisture fluctuations. Boundary-Layer Meteorol. 26:81–93.

Schumann U (1989) Large-eddy simulation of turbulent diffusion with chemical reactions in the convective boundary layer. Atmos Environm. 23:1713–1727.

Sedefian L (1980) On the vertical extrapolation of mean wind power density. J Climate Appl Meteorol. 19:488–493.

Seinfeld JH and Pandis SN (1998) Atmospheric chemistry and physics. Wiley, New York, 1326 pp.

Shaw RH (1985) On diffusive and dispersive fluxes in forest canopies. In: Hutchinson BA and Hicks BB (eds.), The Forest-Atmosphere interaction. Reidel Publishing Company, 407–419.

Siebicke L, Hunner M and Foken T (2012) Aspects of CO_2-advection measurements. Theor Appl Climat. 109:109–131.

Sinclair TR, Allen jr. LH and Lemon ER (1975) An analysis of errors in the calculation of energy flux densities above vegetation by Bowen-ratio profile method. Boundary-Layer Meteorol. 8:129–139.

Skeib G (1980) Zur Definition universeller Funktionen für die Gradienten von Windgeschwindigkeit und Temperatur in der bodennahen Luftschicht. Z Meteorol. 30:23–32.

Smith SD, Fairall CW, Geernaert GL and Hasse L (1996) Air-sea fluxes: 25 years of progress. Boundary-Layer Meteorol. 78:247–290.

Snyder RL, Spano D and Paw U KT (1996) Surface renewal analysis for sensible and latent heat flux density. Boundary-Layer Meteorol. 77:249–266.

Stull RB (1988) An Introduction to Boundary Layer Meteorology. Kluwer Acad. Publ., Dordrecht, Boston, London, 666 pp.

Su HB, Schmid HP, Grimmond CSB, Vogel CS and Curtis PS (2008) An assessment of observed vertical flux divergence in long-term eddy-covariance measurements over two Midwestern forest ecosystems. Agrical Forest Meteorol. 148:186–205.

Tanner CB and Thurtell GW (1969) Anemoclinometer measurements of Reynolds stress and heat transport in the atmospheric surface layer. ECOM, United States Army Electronics Command, Research and Developement, ECOM-66-G22-F, Fort Huachuca, AZ, 82 pp.

Tsvang LR, Zubkovskij SL, Kader BA, Kallistratova MA, Foken T, Gerstmann W, Przandka Z, Pretel J, Zelený J and Keder J (1985) International turbulence comparison experiment (ITCE-81). Boundary-Layer Meteorol. 31:325–348.

Turnipseed AA, Pressley SN, Karl T, Lamb B, Nemitz E, Allwine E, Cooper WA, Shertz S and Guenther AB (2009) The use of disjunct eddy sampling methods for the determination of ecosystem level fluxes of trace gases. Athmospheric Chemistry and Physics. 9:981–994.

Twine TE, Kustas WP, Norman JM, Cook DR, Houser PR, Meyers TP, Prueger JH, Starks PJ and Wesely ML (2000) Correcting eddy-covariance flux underestimates over a grassland. Agrical Forest Meteorol. 103:279–300.

Vickers D and Mahrt L (1997) Quality control and flux sampling problems for tower and aircraft data. J Atm Oceanic Techn. 14:512–526.

Vilà-Guerau de Arellano J (2003) Bridging the gap between atmospheric physics and chemistry in studies of small-scale turbulence. Bull Amer Meteorol Soc. 84:51–56.

Vilà-Guerau de Arellano J and Duynkerke P (1992) Influence of chemistry on the flux-gradient relationships for the NO-O_3-NO_2 system. Boundary-Layer Meteorol. 61:375–387.

Webb EK (1970) Profile relationships: the log-linear range, and extension to strong stability. Quart J Roy Meteorol Soc. 96:67–90.

Webb EK (1982) On the correction of flux measurements for effects of heat and water vapour transfer. Boundary-Layer Meteorol. 23:251–254.

Webb EK, Pearman GI and Leuning R (1980) Correction of the flux measurements for density effects due to heat and water vapour transfer. Quart J Roy Meteorol Soc. 106:85–100.

Wichura B, Buchmann N and Foken T (2000) Fluxes of the stable carbon isotope ^{13}C above a spruce forest measured by hyperbolic relaxed eddy accumulation method. 14th Symposium on Boundary Layer and Turbulence, Aspen, CO., 7–11 Aug. 2000. Am. Meteorol. Soc., Boston, pp. 559–562.

Wieringa J (1980) A revaluation of the Kansas mast influence on measurements of stress and cup anemometer overspeeding. Boundary-Layer Meteorol. 18:411–430.

Wieringa J (1989) Shapes of annual frequency distribution of wind speed observed on high meteorological masts. Boundary-Layer Meteorol. 47:85–110.

Wilczak JM, Oncley SP and Stage SA (2001) Sonic anemometer tilt correction algorithms. Boundary-Layer Meteorol. 99:127–150.

Wrzesinsky T and Klemm O (2000) Summertime fog chemistry at a mountainous site in Central Europe. Atmos Environm. 34:1487–1496.

Wyngaard JC (1981) The effects of probe-indused flow distortion on atmospheric turbulence measurements. J Appl Meteorol. 20:784–794.

Wyngaard JC (1982) Boundary-Layer Modelling. In: Nieuwstadt FTM and Van Dop H (eds.), Atmospheric Turbulence and Air Pollution Modelling. Reidel, Dordrecht, 69–106.

Wyngaard JC and Moeng C-H (1992) Parameterizing turbulent diffusion through the joint probability density. Boundary-Layer Meteorol. 60:1–13.

Wyngaard JC, Businger JA, Kaimal JC and Larsen SE (1982) Comments on 'A revaluation of the Kansas mast influence on measurements of stress and cup anemometer overspeeding'. Boundary-Layer Meteorol. 22:245–250.

Zhang SF, Wyngaard JC, Businger JA and Oncley SP (1986) Response characteristics of the U.W. sonic anemometer. J Atm Oceanic Techn. 2:548–558.